JOC The Journal of Organic Chemistry

pubs.acs.org/joc Article

Experimental and Computational Mechanistic Study of Carbonazidate-Initiated Cascade Reactions

Qinxuan Wang, Jiun-Le Shih, Ka Yi Tsui, Croix J. Laconsay, Dean J. Tantillo,* and Jeremy A. May*

Cite This: https://doi.org/10.1021/acs.joc.2c00696 Read Online

ACCESS | Metrics & More | Article Recommendations | Supporting Information

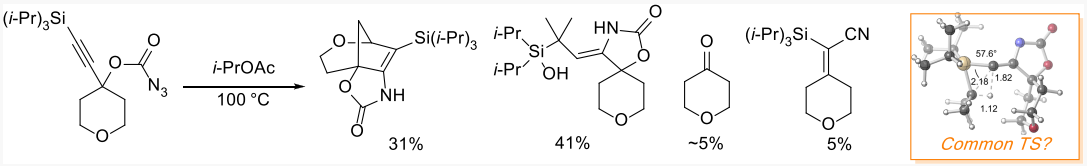

ABSTRACT: A variety of Huisgen cyclization or nitrene/carbene alkyne cascade reactions with different types of termination were investigated. Accessible nitrene precursors were assessed, and carbonazidates were found to be the only effective initiators. Solvents, terminal alkynyl substituents, and catalysts can all impact the reaction outcome. Study of the mechanism both computationally (by density functional theory) and experimentally revealed relevant intermediates and plausible reaction pathways.

INTRODUCTION

Carbenes are neutral, divalent carbon species containing two unshared electrons that play an important role in organic synthesis due to their high and divergent reactivity.[1] Electrophilic carbenes, such as those derived from diazocarbonyl compounds by catalysis, thermolysis, or photolysis, provide numerous useful transformations in organic synthesis.[2] The reaction types include, but are not limited to, Wolff rearrangement,[3] cyclopropanation,[4] C−H insertion,[5] X−H insertion,[6−8] Buchner reaction,[9] and ylide formation,[10] giving chemists a powerful tool to build C−C and C−X bonds. Current efforts in the development of carbene-based methods focus on the synthesis of difficult atomic structures at the core of important molecules.

Heteroatom-containing polycyclic structural motifs can be found in many biologically active natural products. Of these motifs, two important examples are bridged polycycles and propellanes. Carnosol,[11] maoecrystal V,[12] harringtonolide,[13] ialibinone A,[14] and gelsemine[15] are examples of natural products that include a bridged polycyclic motif (Figure 1). Propellanes are tricyclic compounds in which the three rings share a common C−C single bond.[16] Brazilide A,[17] lapidilectine B,[18] isoschizogamine,[19] and batrachotoxin A[20] are examples of natural products which contain propellane structures.

Many diverse strategies for the construction of bridged polycycles have been explored. The Diels−Alder reaction has been a common strategy used for the synthesis of the bridged bicyclo[2.2.2]octane core (**2**) of maoecrystal V (Scheme 1a).[21] However, this approach is not applicable to all bridged ring isomers. For example, it would not be able to produce the bicyclo[3.2.1]octane isomer (**4**) via 1,4-diene **3**. In comparison, a general methodology that started from easily accessible precursors via carbene intermediates by utilizing C−H

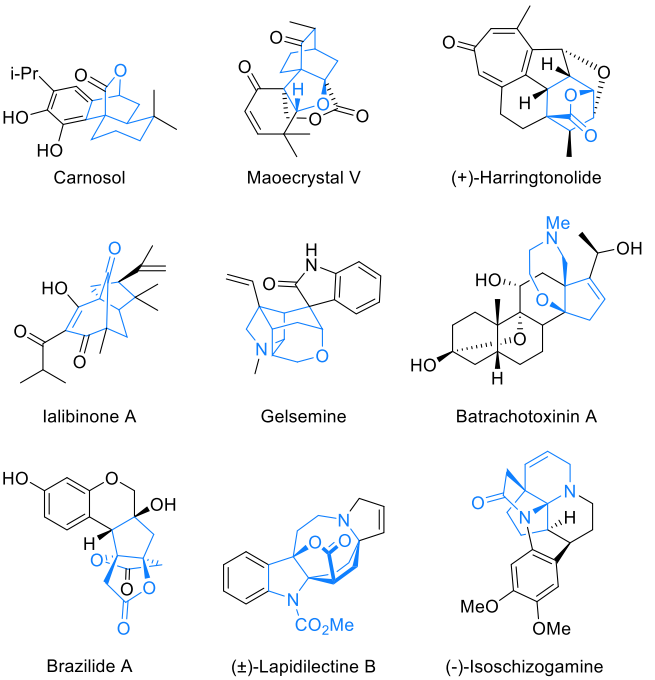

Figure 1. Examples of natural products with bridged polycycles and propellanes.

Received: March 26, 2022

Scheme 1

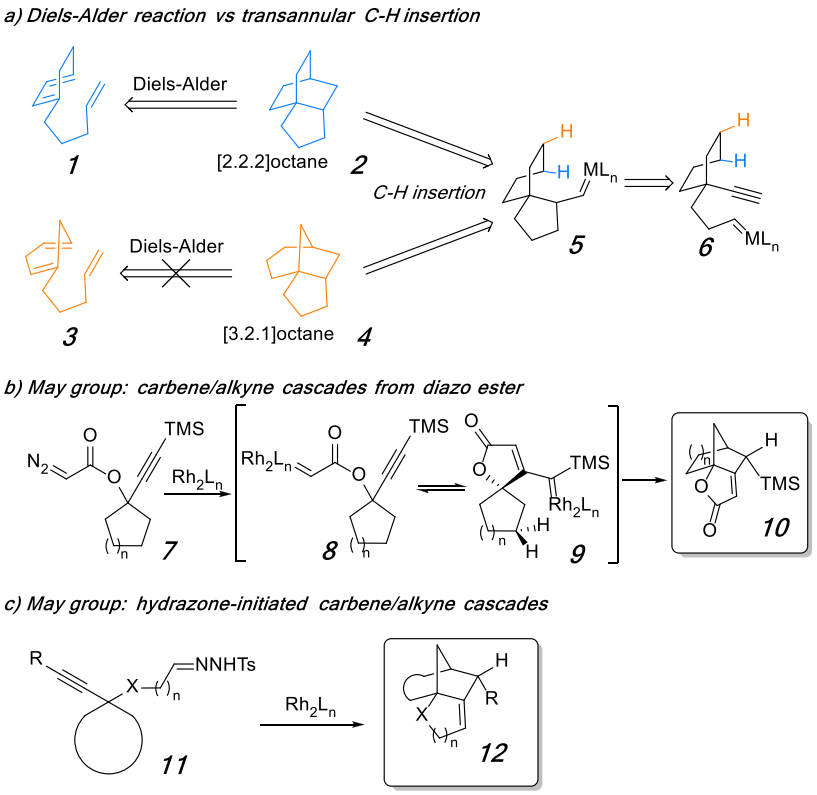

(A) Comparison of Diels−Alder vs Carbene-Initiated Cascade Reaction Synthetic Strategies for Bridged Polycyclic Rings. (B) Carbene/alkyne cascades in synthesis. (C) Proposed approach for nitrene/alkyne cascades in synthesis.

insertion to construct bridged polycycles would be more universal. Thus, our group and others have developed a variety of carbene/alkyne cascade reactions for the synthesis of polycycles.[22,23]

Carbene/alkyne cascades were initially explored by the Hoye[23a] and Padwa[23b] groups. Recently, our group reported a series of cascade reactions that terminated in C−H bond insertion after catalytic diazo decomposition of an α-diazo ester **7** and carbene/alkyne metathesis to synthesize bridged polycycles **10** (Scheme 1b).[22a] Thus, multiple C−C bonds and multiple rings were formed in a single reaction step. Hydrazone-initiated carbene/alkyne cascades from diazoalkanes **11** also produced a variety of bridged polycycles **12** with carbocyclic rings fused to the bridged core.[22b] In addition, many other carbene cascade-based methods have been reported in recent years.[23c−e]

Nitrogen, as found in several natural products, is particularly relevant to biological activity; however, nitrogen-containing targets often present significant synthetic challenges. Nitrene/alkyne cascades, which start from alkynyl-bound nitrene precursors, can rapidly build *N*-heterocyclic compounds, usually in only one step.[24] Therefore, the selective synthesis of bridged azacycles through this method caught our attention. To this end, we planned to investigate the possibilities of using different nitrogen-containing substrates to achieve bridged azacycles. By using different nitrene precursors to **13**, a variety of *N*-heterocyclic compounds **15** could then be synthesized chemoselectively (Scheme 2).

Computational Methods.[25] Density functional theory (DFT) calculations were performed using Gaussian 16.[26] Without geometrical constraints, optimization and frequency

Scheme 2. Designed Nitrene-Initiated Cascade Reactions

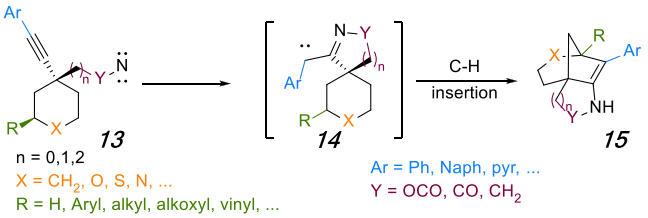

calculations for all structures were performed at the CPCM-(dichloromethane)-ωB97XD/6-311++G(d,p)[27,28] level for all intermediates and transition-state structures (TSSs). Individual TSSs were confirmed by both a relevant imaginary frequency and intrinsic reaction coordinate (IRC) calculations.[29] All singlet and triplet structures were optimized with an unrestricted wavefunction with the keyword guess=(mix,always).

RESULTS AND DISCUSSION

Investigation of Outcomes from Phenyl Alkyne-Appended Alkyl Azides and Amides. Initial trials of potential nitrene initiators, such as alkynyl alkyl azide **16** (Table 1), yielded no cascade products in any of the reactions. The azides were unreactive at room temperature, even in the presence of a rhodium catalyst (entries 1 and 2). Increasing the reaction temperature led to triazole **17** that was generated by a [3 + 2] Huisgen cycloaddition (entries 3 and 4). Dinitrogen extrusion did not occur after the formation of the triazoles, even in the presence of $Rh_2(esp)_2$.

https://doi.org/10.1021/acs.joc.2c00696
J. Org. Chem. XXXX, XXX, XXX−XXX

Table 1. Cascade Reaction of Alkyl Azides

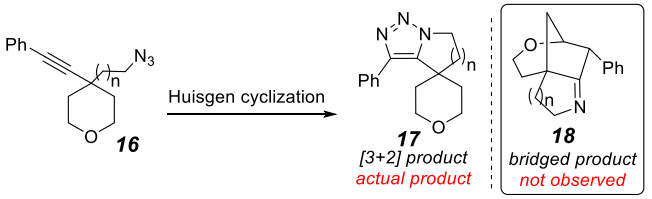

entry	n	catalyst	additive	solvent[a]	temp.	result
1	2	none	none	DCE[b]	rt[b]	>95% S.M. recovered[c]
2	2	$Rh_2(esp)_2$[b,d]	none	DCE	rt	>95% S.M. recovered[c]
3	2	none	none	toluene	reflux	**17a**, 77% yield
4	1	$Rh_2(esp)_2$[d]	4 Å M.S.[e]	toluene	reflux	**17b**, 73% yield

[a]0.1 M for azide **16**. [b]Abbreviations: $Rh_2(esp)_2$ = $Rh_2(\alpha,\alpha,\alpha',\alpha'$-tetramethyl-1,3-benzenedipropionate). DCE = 1,2-dichloroethane. rt = room temperature (~20 °C). [c]>95% of the starting material was recovered. [d]5 mol %. [e]Molecular sieves were added. See the Supporting Information for more details.

Amide **19** was also tested as a nitrene precursor with typical conditions (Scheme 3). When using $Rh_2(esp)_2$ as the catalyst in the presence of $PhI(OAc)_2$ and MgO, the Curtius rearrangement product acetamide **20** was produced in 86% yield. With the alternative oxidant $PhI(OPiv)_2$ and the additive CaO,[30] the corresponding pivalamide **21** was obtained in 47% yield along with a urea product **22** in 36% yield. The formation of both the amides and the urea revealed that, after nitrene generation, a Curtius rearrangement was faster than the nitrene/alkyne metathesis reaction.

These early studies showed the scope and importance of cascade initiation and are important controls that show the importance and unique reactivity of the carbonazidate functional group, as discussed below. For example, **16** and **17** show the feasibility of the Huisgen cyclization, but a discrete nitrene intermediate would be operative for the Curtius rearrangement of amide **19**. The carbonazidate could follow either of these initiations, which is what prompted the more detailed studies that follow.

Investigation of Silanol and Vinyl Nitrile Formation from Silyl Alkyne-Appended Carbonazidates and Mechanistic Study. During the development of Huisgen cyclization/carbene cascade reactions from carbonazidates, we found that a silyl alkynyl carbonazidate like **24** (Scheme 4a) can form the anticipated bridged tricyclic product **25** in 31% yield, which illustrated that the carbonazidate could be used as an effective starting material for the construction of bridged azacycles.[31] However, an unusual silanol product **26** was isolated as the major product in 41% yield. The reaction also generated two different byproducts: tetrahydropyranone **27** and silyl vinyl nitrile **28**. We did not observe silanol product **26** in the NMR of the crude reaction material; instead, azasilacyclopentene **34** (Scheme 4b) was determined to be the reaction product before an aqueous workup caused silanol formation by hydrolysis of the Si−N bond. Therefore, we proposed the mechanism for the formation of silanol **25** and bridged tricycle **26** shown in Scheme 4b. Carbonazidate **24** can first undergo Huisgen cyclization to form triazole **29**. Then, α-imino carbene **30** can be generated via ring opening of triazole **29**, followed by extrusion of nitrogen. After carbene generation, a C−H bond insertion occurs with the ether-activated methylene (H^a), building the bridged iminyl-tricycle **32** and subsequent tautomerization via a proton transfer to form the bridged enamine-tricycle **25**. Alternatively, tertiary C−H bond insertion on the isopropyl silyl group (H^b) leads to the formation of a kinetically unstable silacyclopropane **33**, which could rearrange in a pseudo-sigmatropic fashion to azasilacyclopentene **34**. The weak Si−N bond in azasilacyclopentene can undergo rapid hydrolysis and give silanol **26**. Validating these proposed mechanistic steps and the unexpected C−C bond fragmentation seen in **27** and rearrangement seen in **28** prompted further mechanistic investigation.

To verify our proposed mechanisms, DFT calculations were performed. Our calculations predicted that the ground state for **31** is a triplet state, **31** (**T**), which is 6.4 kcal mol^{-1} lower in energy than the singlet state, **31** (**S**). Accurately computing S−T gaps is a known challenge for the current theoretical methods due to the energetic proximity between the two states and the difficulties in fair comparison of the open- and closed-

Scheme 3. Amide-Initiated Cascades

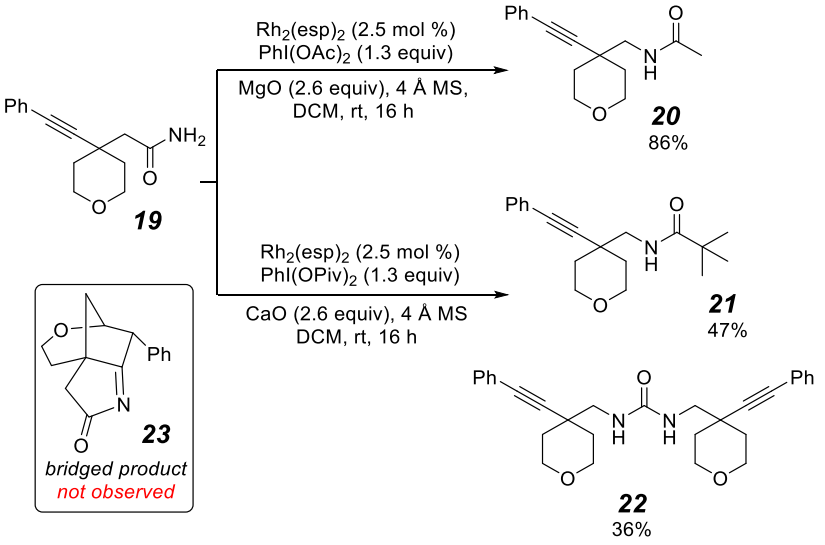

https://doi.org/10.1021/acs.joc.2c00696
J. Org. Chem. XXXX, XXX, XXX−XXX

Scheme 4

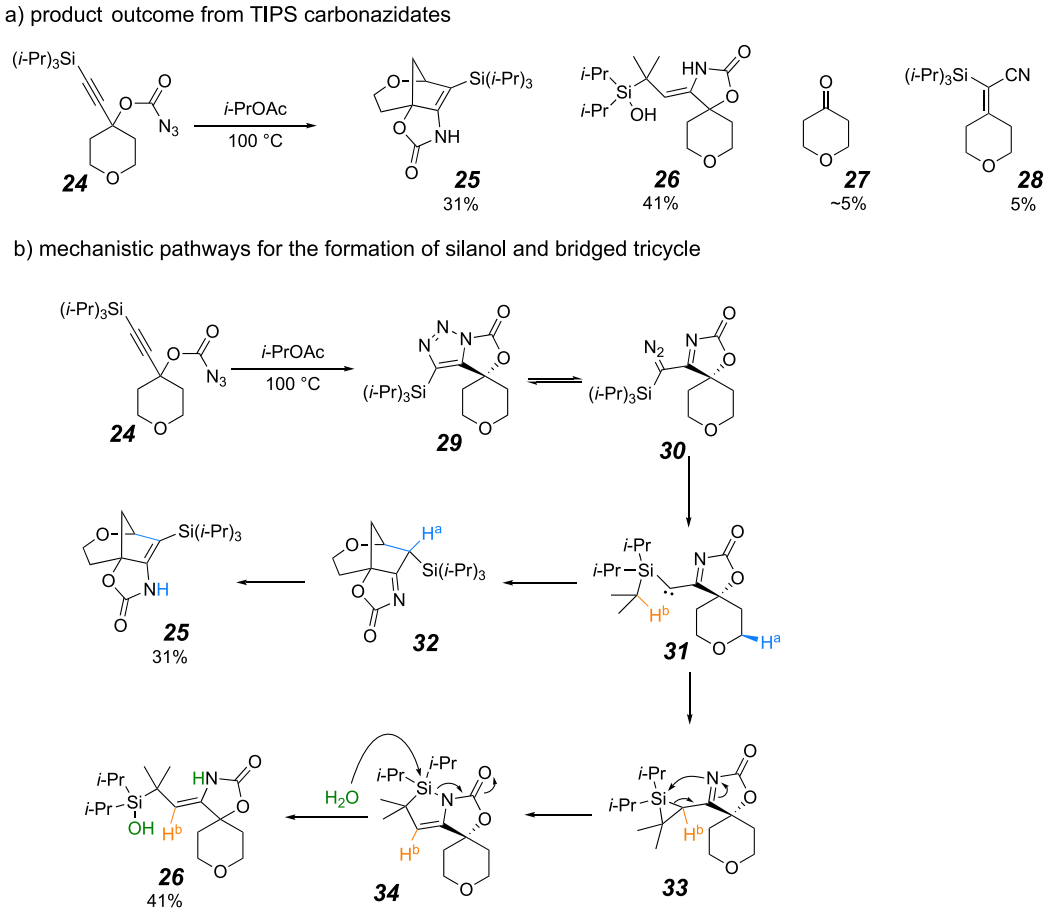

(A) Multiple Products Obtained from a Carbonazidate-Initiated Cascade Reaction of TIPS-Alkynyl Carbonazidates. (B) Early proposed mechanisms for the formation of multiple products.

shell systems. Therefore, while we urge caution in assigning high confidence to the ~6 kcal mol^{-1} S−T gap for **31** (and **47**) in a quantitative sense, we are fairly confident that the qualitative trend, the triplet state(s) of **31** (and **47**) is favored, is correct for the carbenes reported.[32,33] Here, we selected a DFT method since it includes correlation within a self-consistent field formalism and has less spin contamination, but calculations of S−T with DLPNO-CCSD(T) give qualitatively similar results (see the Supporting Information).[31] The performance of DFT methods in calculating S−T gaps also has been assessed in previous studies.[34] Here, our analysis set the free energy of **31** (**T**) as the relative zero. There are several sites in **31** where the carbene center C_4 can react intramolecularly. First, we discuss the C_4 insertion into C_{10}−H^a with a barrier (singlet) of 7.4 kcal mol^{-1} (see numbering in Scheme 4 and Figure 2). This leads to the formation of a bridged iminyl-tricyclic intermediate **32** (**S**). Solvent-assisted proton transfer of **32** (**S**) leads to the enamine-tricyclic product **25** (**S**), which is 54.3 kcal mol^{-1} downhill relative to **31** (**T**)—a TSS for solvent-assisted proton transfer was not modeled here. Alternatively, C_4 can insert into C_3−H^b with a barrier (singlet) of 18.9 kcal mol^{-1}, which results in the formation of a silacyclopropane intermediate **33** (Scheme 4 and Figure 2). Through a pseudopericyclic [1,3] sigmatropic shift,[35] **33** (**S**) forms **34** (**S**) with a barrier of 11.3 kcal mol^{-1} (Figure 2). Subsequently, water can add to **34** (**S**), followed by a solvent-assisted tautomerization, forming **26** (**S**). Based on the calculated barriers, we predicted that the formation of **26** (**S**) is thermodynamically favored over **25** (**S**), but formation of **25** (**S**) is kinetically favored over **26** (**S**).

We have also considered these mechanisms on the triplet surface, but the triplet versions of all intermediates in Figure 2 have consistently higher free energies. Predicted barriers (see the Supporting Information for details) also exceed the limit to be kinetically feasible under the current experimental conditions. Thus, it is likely that **31** (**T**) has to be excited to **31** (**S**) to form **25** (**S**) and **26** (**S**). However, we also cannot eliminate the possibility of surface crossing elsewhere along the reaction paths.

Mechanisms for formation of ketone **27** and silyl vinylnitrile **28** are still unclear. In our original communication, we proposed the formation of a highly strained bicyclic azirine intermediate **35** via electrocyclization of α-imino carbene **31** (Scheme 5a). An internal C−N bond fragmentation led to the ring-expanded product **36**. Two pathways could follow: (a) C−C bond fragmentation to provide ketone **27** (path A); (b) decarboxylation via a retro-hetero Diels−Alder reaction followed by a 1,2-silyl migration to yield the silyl vinylnitrile **28** (path B).

To more fully understand the mechanism for the formation of all observed products, we investigated possibilities via computational methods (Scheme 5b and Figure 3). However, **36** (**S**) failed to optimize as a minimum on the potential energy surface. Although **36** (**T**) is predicted to be a minimum (ΔG =

https://doi.org/10.1021/acs.joc.2c00696
J. Org. Chem. XXXX, XXX, XXX−XXX

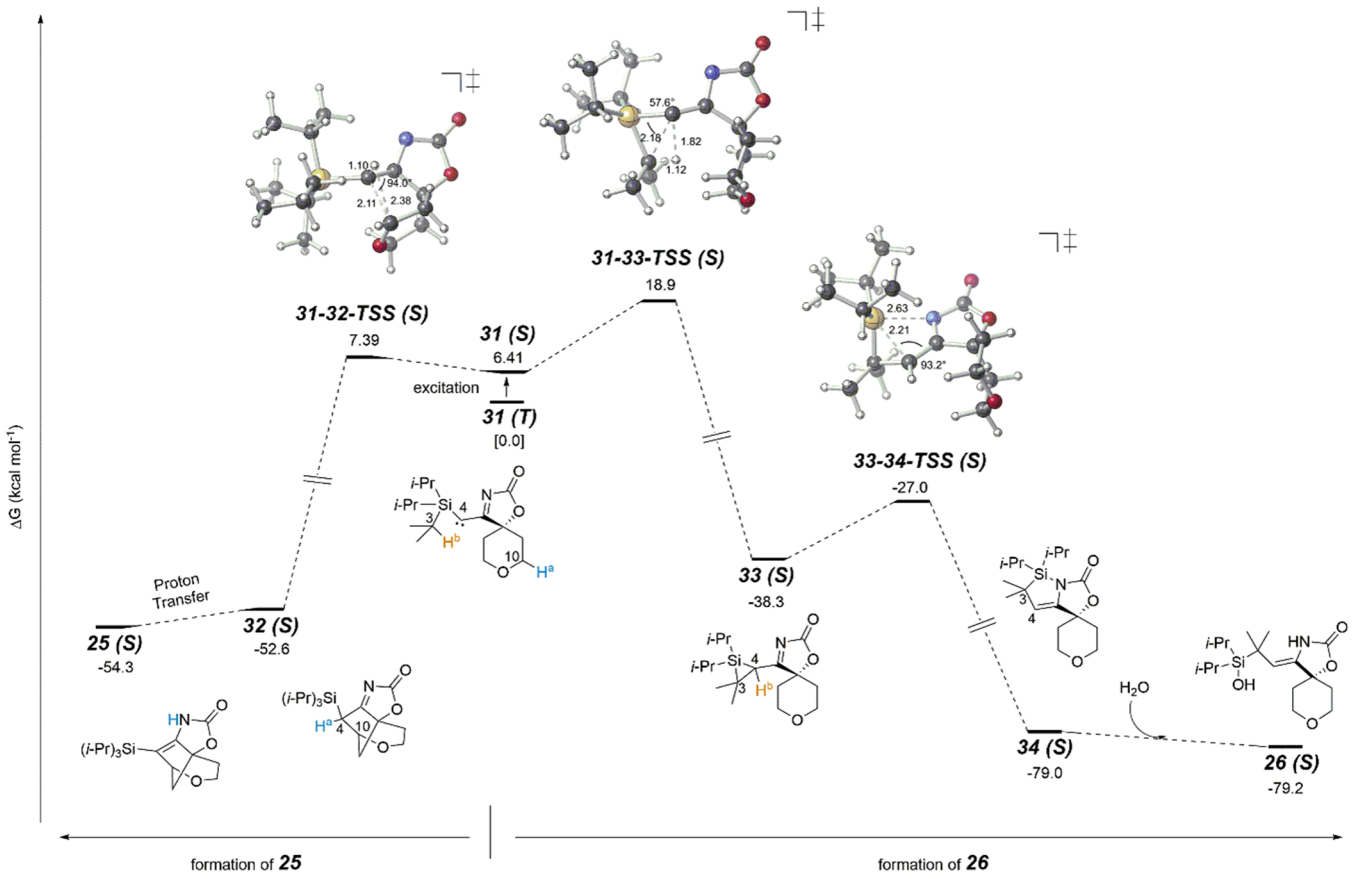

Figure 2. Free-energy diagram for mechanisms forming **25 (S)** (left) and **26 (S)** (right). Energies are reported in kcal mol^{-1} but not drawn to scale. Only singlet TSSs and intermediates are reported here. Triplet versions of these structures were also considered, but their calculated barriers exceed the limit of kinetic feasibility under the given reaction temperature (see the Supporting Information for details).

18.8 kcal mol^{-1}), we failed to identify any TSS from carbene **31 (T)** to **36 (T)** by scanning the potential energy surface. This led us to an alternative mechanism which does not involve **36 (S)**. In this pathway (path B′), **31 (S)** forms **35 (S)** endergonically with a predicted barrier of 18.0 kcal mol^{-1}. Starting from path A, we were able to identify a TSS from **35 (S)**, which leads to **27 (S)** and **27a (S)**, but the predicted barrier is 55.1 kcal mol^{-1}, much too high for the reaction temperature used (Figure 3a). We failed to identify any energetically viable mechanism from **35 (S)** to **27 (S)**. Alternatively, **31 (S)** can fragment directly to **27 (S)** and **27a (S)** in a single step with a predicted barrier of 12.9 kcal mol^{-1}. Therefore, **27 (S)** may be formed directly from **31 (S)** instead of **35 (S)**. **27a** is unusual because of its ethyne isocyanate substructure. Alkynyl isocyanates have been previously synthesized and characterized[36] and are relevant to polymer chemistry, atmospheric chemistry, and interstellar chemistry.[33,37] Here, we expect **27a** to react further and possibly contribute to the formation of other side products.

For path B, the lowest-energy computed pathway for the formation of the silyl vinylnitrile **28** proceeds through a vinylidene carbene intermediate **39**, which can react with silyl nitrile **40** via Si−C bond insertion (Figure 3b). More specifically, we propose that **35 (S)** first undergoes decarboxylation to form **38 (S)**, with a predicted barrier of 18.5 kcal mol^{-1} (Figure 3, bottom). In an endergonic step, **38 (S)** then dissociates into an unsaturated carbene **39 (S)** and a nitrile **40 (S)**. Although unsaturated carbenes are known to undergo rearrangement, for example, vinylidenes isomerize to alkynes,[12] we suspect that such a transformation is infeasible for **39** due to the resulting increase in ring strain. Instead, **39 (S)** can combine with **40 (S)** to form **28 (S)**. However, the overall barrier for path B is predicted to be 44.3 kcal mol^{-1} from **38 (S)** to **39-28-TSS (S)**, again too high for the reaction conditions used. An alternative mechanistic pathway was computed, but it resulted in an even higher (75.5. kcal mol^{-1}) predicted barrier relative to **31 (T)**—it could be that an energetically allowed spin surface crossing occurs on the way to product **28 (S)**, but so far, strong evidence for that remains elusive (see the Supporting Information, Figures CS2-4). Known synthetic methods were attempted to try and replicate vinyl nitrile formation[38] but failed.

In order to avoid the insertion at the α-silyl C−H bonds and force bridged bicycle formation, a reaction with *tert*-butyldiphenyl silylacetylene carbonazidate **41** was tested, from which five products were isolated (Scheme 6a). The α-diazo oxazolone **43** was proven to be an intermediate in this Huisgen cyclization/carbene cascade reaction since purified **43** can form ketone **44**, vinyl nitrile **45**, and silanol **46** when heated in dichloroethane. The formation of silanol **46** appeared to proceed through a 1,2-phenyl migration. Previously, we proposed that after 1,2-phenyl migration in α-imino carbene **47**, the silanol product **46** was produced from imine **49** by hydrolysis (Scheme 6b). However, computations suggested that an alternative Si−N cyclobutene containing intermediate **50** would be ∼30 kcal mol^{-1} lower in energy than imine **49**, which would add water to give product **46**.

https://doi.org/10.1021/acs.joc.2c00696
J. Org. Chem. XXXX, XXX, XXX−XXX

Scheme 5

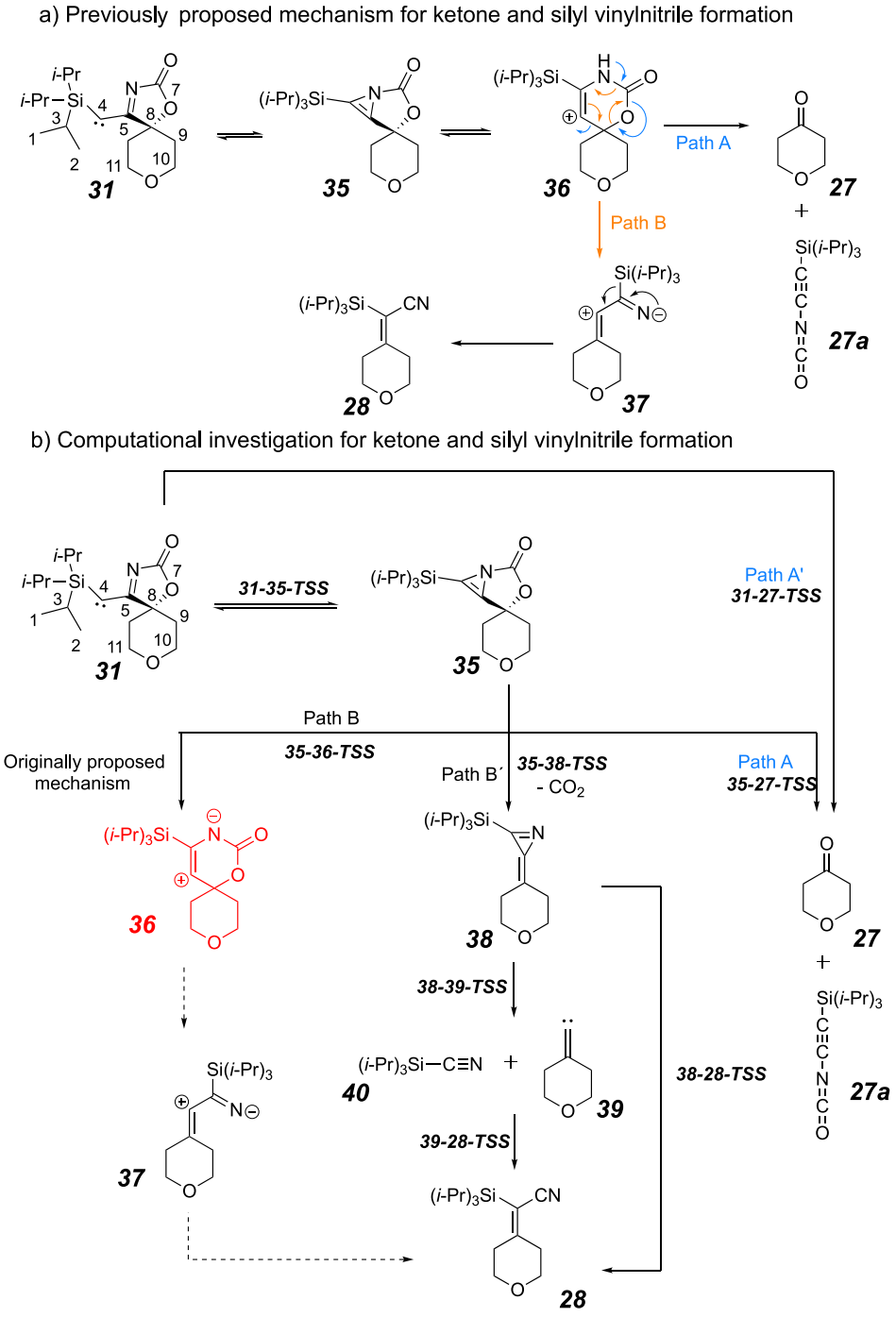

(A) Possible Mechanistic Pathways for the Ketone **27** and Vinyl Nitrile **28** Formation. See Figure 3 for transition-state energies. (B) Pathways investigated in our calculations. The carbon backbone is numbered **31**.

From **47**, two mechanistic pathways were considered that led to **46** (Figure 4): (1) a pathway on the carbene singlet surface (accessed by initial excitation; Figure 4, pathway in blue) and (2) a pathway on the carbene triplet surface (Figure 4, black) from the ground state of **47**. The results of our calculations predict that the former is overall energetically favored over the latter, but we describe below why neither can be ruled out completely simply based on the energies—in other words, both pathways are possible and could be simultaneously operative.

Silanol **46** can be formed via the singlet pathway (in blue) following excitation of **47 (T)** to the singlet surface (**47 (S)**, 6.3 kcal mol^{-1}). **48-TSS** exists on both the singlet and triplet surfaces, and these two TSSs differ by 21 kcal mol^{-1}, favoring the singlet pathway (i.e., 8.5 kcal mol^{-1} vs 30.2 kcal mol^{-1}, both relative to ground-state **47**). Whereas **48-TSS (S)** leads to the Si−N cyclobutene intermediate **50 (S)** by an IRC calculation,[28] the analogous **48-TSS (T)** leads directly to the imine intermediate **49 (T)**, which then leads directly to **46 (T)** after addition of water. Intermediate **50 (S)** is predicted to face a barrier of 32.8 kcal mol^{-1}; however, in both the singlet and

https://doi.org/10.1021/acs.joc.2c00696
J. Org. Chem. XXXX, XXX, XXX−XXX

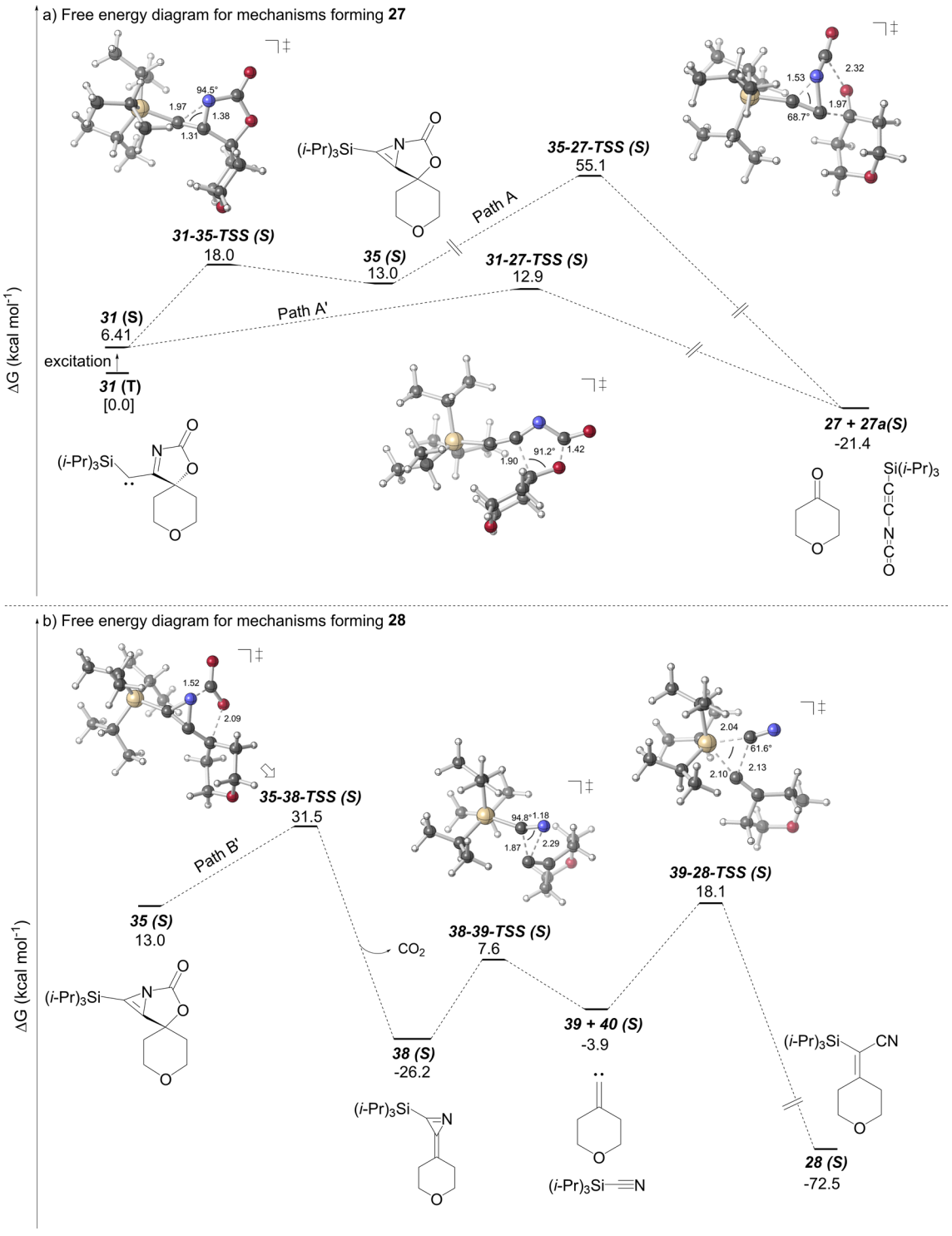

Figure 3. Free-energy diagram for mechanisms forming **27** (**S**) (A, top) and **28** (**S**) (B, bottom). Free energies are reported in kcal mol^{-1} but not drawn to scale. Only singlet TSSs and intermediates are reported. Triplet versions of these structures were also considered, but their calculated barriers exceed the limit of kinetic feasibility under the given reaction temperature (see the Supporting Information for details).

triplet pathways, a barrier of approximately 30 kcal mol^{-1} must be overcome. Formation of alternative product **44** can be explained by a one-step process, wherein a C−C bond fragmentation occurs for **47** (**S**) to form **44** (**S**) and an unusual, linear fragment, **44a**, that we suspect goes on to form undesired side products (Figure 4, left).

To garner experimental support for the mechanism that was based on our calculations, an NMR study was performed using a ^{15}N-labeled carbonazidate ^{15}**N-41** in $CDCl_3$ at 75 °C under extremely anhydrous conditions (Figure 5a). The ^{13}C NMR spectrum showed that intermediate α-diazo oxazolone ^{15}**N-43** was formed after 40 h and then consumed after 180 h (Figure 5b). All of the expected products were observed in the finished reaction prior to exposure to water without any formation of silanol ^{15}**N-46**. After 180 h, the ^{15}N NMR peak with the greatest area appeared slightly downfield from the starting

https://doi.org/10.1021/acs.joc.2c00696
J. Org. Chem. XXXX, XXX, XXX−XXX

Scheme 6

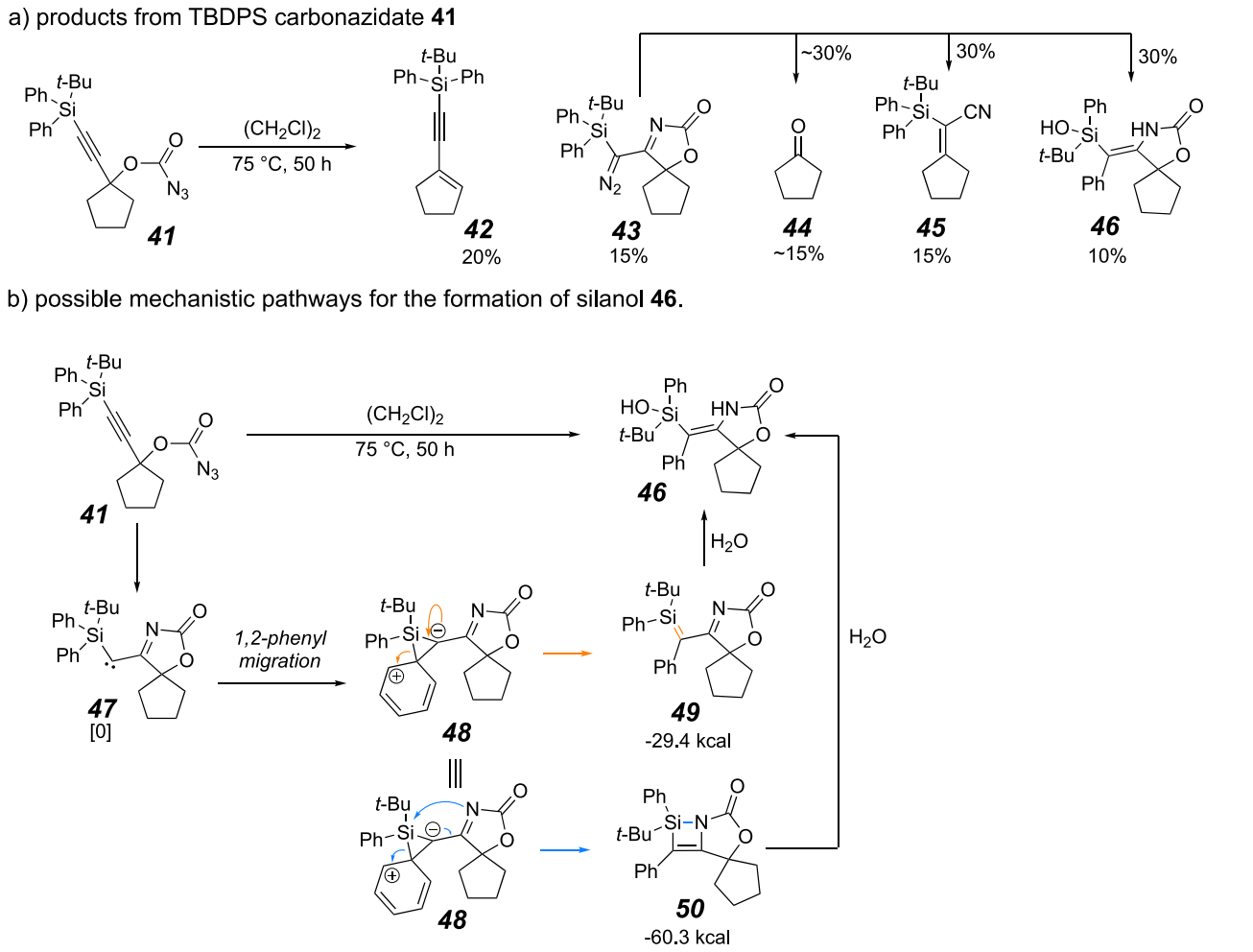

(A) Multiple Products from the Cascade Reaction of a *tert*-Butyldiphenylsilyl Carbonazidate. (B) Possible mechanistic pathways for the formation of multiple products.

carbonazidate (Figure 5c). After exposing the reaction mixture to wet air, the peak disappeared, and a new peak that corresponded to silanol ^{15}**N-46** appeared further upfield than the intermediate peak. Consequently, it appeared that the transient peak at δ = 112.8 ppm belonged to the product of the reaction before water addition, which would be ^{15}**N-49** or ^{15}**N-49**. The chemical shift of ∼112 ppm matches the reported values for enamine structures[39] but not for imines.[40] We also noticed that there was a relatively small peak at δ = 305.9 which could have been from an imine product. These results strongly suggested that the Si−N cyclobutene containing enamine ^{15}**N-50** is more likely to be the most abundant intermediate before water addition, consistent with the computational results. The trace amount of imine formation also indicated that an equilibrium might exist between imine ^{15}**N-49** and enamine ^{15}**N-50** that favors the latter, which is also corroborated by computational results (**50** (***S***) is energetically favored over **49** (***S***) by 27 kcal mol^{-1}).

Formation of vinyl nitrile **45** is predicted by our calculations to involve a more complex energetic landscape. Upon excitation of **47** to the singlet surface, azirine **51** (**S**) can form in a step predicted to be endergonic by 14.1 kcal mol^{-1} (Figure 6). Then, **51** (**S**) can decarboxylate, leading to azirine intermediate **52** (**S**), which is then predicted to fragment to vinylidene **53** and nitrile **54**. Recombination is predicted to have only a 13.6 kcal mol^{-1} barrier to product **45**. The overall predicted barrier (an energy difference between **53-45-TSS** and **52**) is 40.5 kcal mol^{-1}, which is likely kinetically infeasible under the reaction conditions used. We pursued alternative mechanisms for the formation of **45** but found none with barriers lower than the overall barrier reported in Figure 6 (see the Supporting Information).

Numerous attempts to find reasonable mechanisms for the formation of **28** and **45** from **31** (***T***) and **47** (***T***), respectively, demonstrate the major challenges that face the discovery of mechanisms based solely on chemical intuition in computational mechanistic organic studies such as these (see the Supporting Information). Computational tools beyond intuition-driven discovery, such as automated reaction path exploration, have been valuable for smaller systems,[41] but applying such methods to complex systems like the one discussed here is beyond the scope of this study. Thus, limited by our intuition, creativity, and computing time, a reasonable mechanism that explains the formation of **28** and **45** remains elusive.

Investigation of Azacycle Formations from Phenyl Alkyne-Appended Carbonazidates. To avoid α-silyl C−H bond insertion and alkyl and aryl migration, we prepared

https://doi.org/10.1021/acs.joc.2c00696
J. Org. Chem. XXXX, XXX, XXX−XXX

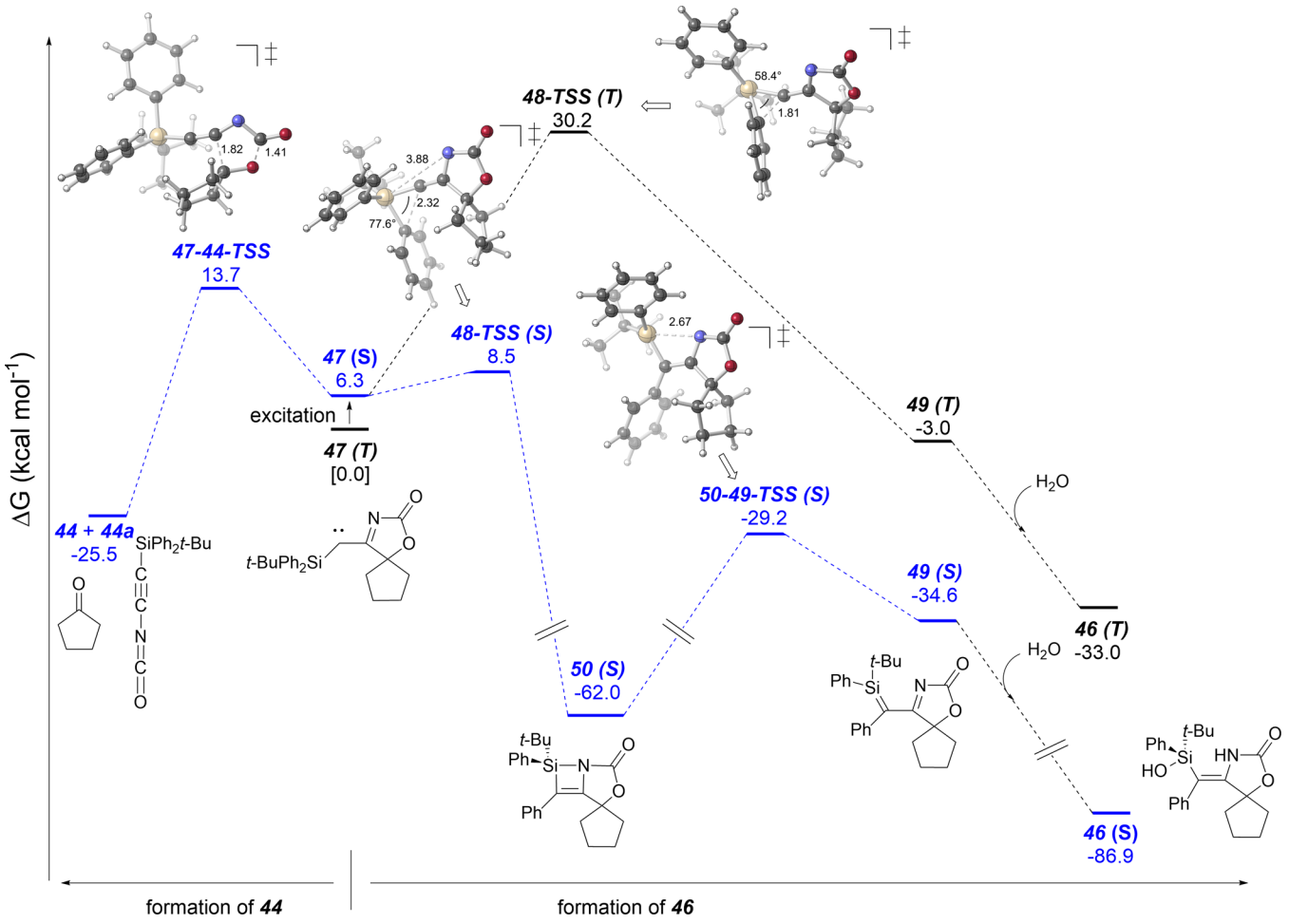

Figure 4. Free-energy diagram for mechanisms forming **46 (S)** (blue right), **46 (T)** (black), and **44 (S)** (blue left). Free energies are reported in kcal mol^{-1} and not drawn to scale.

phenylethynyl carbonazidates, such as **55**, for the cascade reaction (Table 2). Our initial trials quickly showed that the temperature of the thermolysis is very important; higher temperatures caused elimination to form an enyne, while at lower temperatures (below 100 °C), no reaction occurred. Interestingly, different solvents for this cascade reaction result in different ratios of the bridged tricycle **56** to propellane **57**. In line with previous observations,[22] the bridged tricyclic product **56** can easily rearrange with trace acid or base to propellane **57**. Polar aprotic solvents, such as MeCN, showed a high propellane selectivity (entry 1). Nonpolar solvents such as benzene provided some preference for the bridged tricycle (entry 2). Cyclohexane was the most selective for the formation of the bridged tricycle **56** (entry 5). In addition, increasing the concentration inverted the selectivity for propellane **57** over the bridged tricycle **56**, suggesting that the rearrangement may undergo an autocatalytic process (entries 4 and 5).

To assess the propensity for rearrangement to the propellane, carbonazidates with different heterocyclic rings were also investigated for the cascade reaction.[22d] When the oxygen atom of **55** was replaced by an *N*-*t*-butyloxycarbonyl (*N*-Boc) group in the starting material, bridged tricyclic product **59** was produced from carbonazidate **58** without rearrangement (Scheme 7a). Due to the facile rearrangement of bridged azacycles such as **55** with a heteroatom connected to the bridgehead carbon, their purification was quite difficult. One way to extend the shelf life of these bridged structures is by making relatively more stable *N*-Boc-protected bridged tricycles such as **60** (Scheme 7b). To form propellane structures such as **57** exclusively, simple acidification after the cascade reaction can be utilized to achieve that goal (Scheme 7c).

We also tried to use cycloalkyl-containing alkynyl carbonazidates as starting materials to avoid rearrangement. However, the synthesis of the starting carbonazidates was impeded by the preferential formation of the corresponding enynes **63** via elimination (Scheme 8). The failed syntheses of cyclohexyl alkynyl carbonazidates from the corresponding alcohols suggested that the *trans*-diaxial elimination of tertiary cycloalkyl carbonazidate **62** is facile.[22d] To avoid elimination, one strategy was to bias the substrate to maintain the carbonazidate group in an equatorial position (i.e., the conformation seen in **61**). *Cis*-substituted propargyl cyclohexanol **64** could be generated by the axial nucleophilic attack of phenylacetylide **66** on 3-substituted cyclohexanone **65**, and this propargylic alcohol could be converted to carbonazidate **61**. The substituent at the 3-position, trans to the alkyne, would also activate the methine C−H bond for insertion. After the Huisgen cyclization and dinitrogen extrusion from **67**, an α-imino rhodium carbene **68** could be generated in a favorable conformation for a transannular C−H insertion into the

https://doi.org/10.1021/acs.joc.2c00696
J. Org. Chem. XXXX, XXX, XXX−XXX

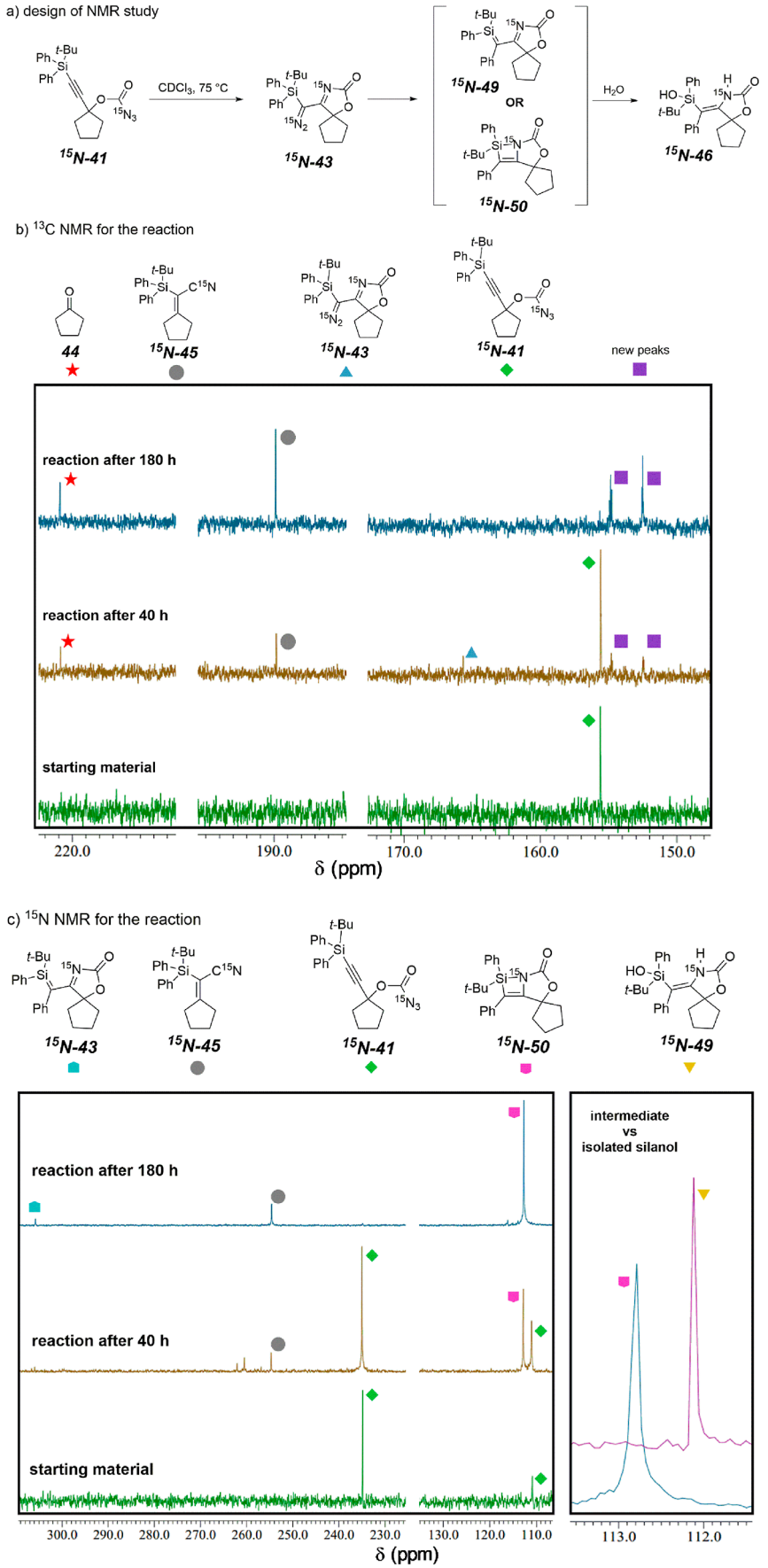

Figure 5. NMR study for mechanisms forming **46**. (A) Possible ^{15}N-labeled mechanistic intermediates. (B) ^{13}C NMR during reaction progress with peaks labeled for reaction intermediates. (C) ^{15}N NMR during reaction progress with peaks labeled for reaction intermediates.

https://doi.org/10.1021/acs.joc.2c00696
J. Org. Chem. XXXX, XXX, XXX−XXX

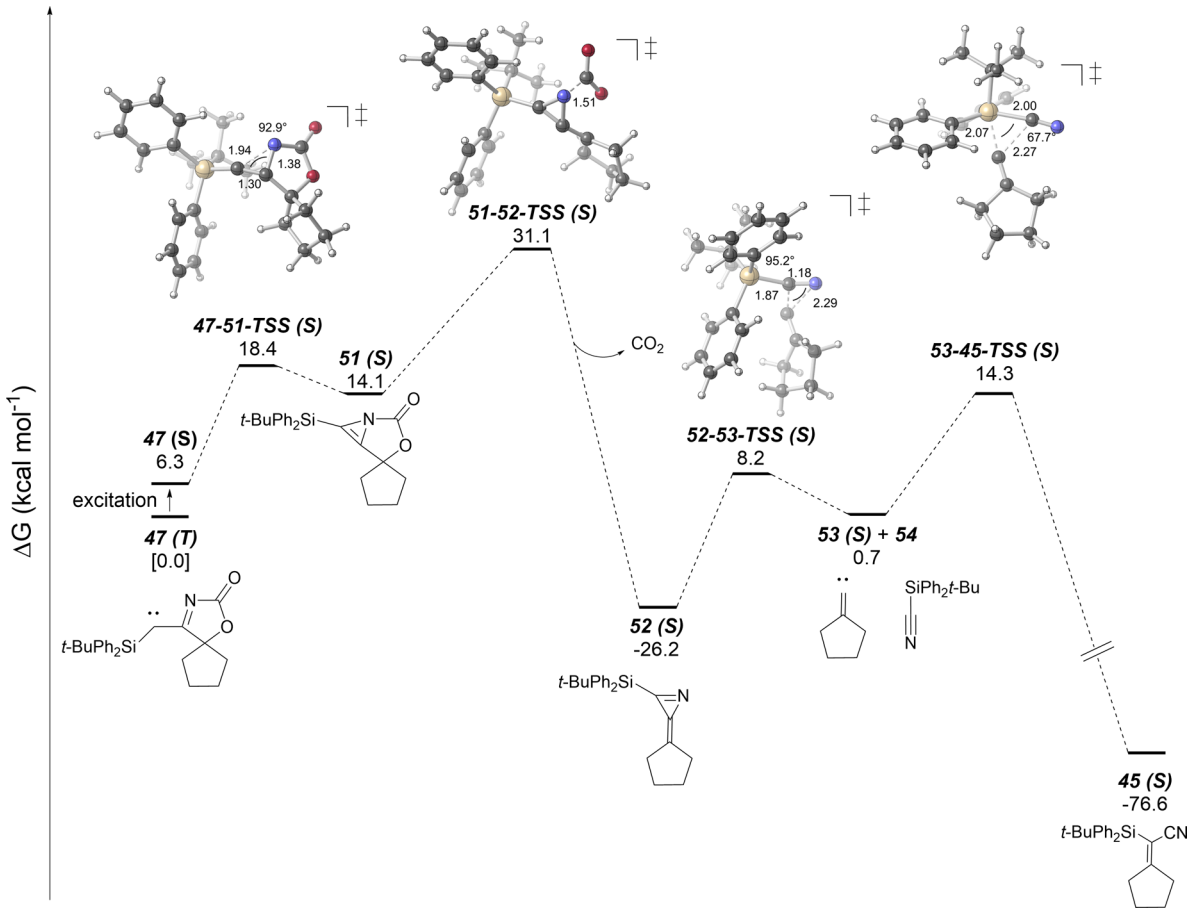

Figure 6. Free-energy diagram for mechanisms forming **45 (S)**. Free energies are reported, and units are in kcal mol^{-1}. Energies are not to scale. Only singlet TSSs and intermediates are reported here. Triplet versions of these structures were also considered, but their calculated barriers exceed the limit of kinetic feasibility under the given reaction temperature (see Supporting Information for details).

Table 2. Formation of Bridged Tricycle 56 vs Propellane 57

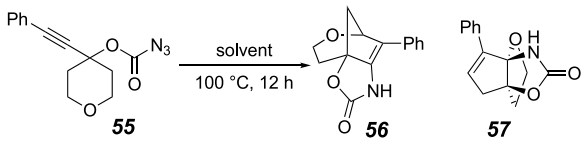

entry	solvent	conc.[a]	ratio of 56:57[b]
1	MeCN	0.02 M	<1:99
2	benzene	0.02 M	3.7:1
3	*i*-PrOAc	0.02 M	8.3:1
4	cyclohexane	1.0 M	1:22
5	**cyclohexane**	**0.02 M**	**17:1**

[a]Concentration of carbonazidate **55**. [b]Ratio determined by ^{1}H NMR analysis of peak integrations.

activated methine, which leads to the bridged tricycle **69**. To our delight, the yield of bridged azacycle increased to greater than 70% when carbene insertion occurred at a tertiary, benzylic, or allylic C−H bond.

Investigation of Alternate Outcomes from Phenyl Alkyne-Appended Carbonazidates with Different Solvents. During the solvent screen for phenylethynyl carbonazidates, we found out that when hydrocarbons such as hexane or cyclohexane were used as solvents, ketone byproducts were formed (e.g., **58** to **70**, Scheme 9a). However, when the solvent was changed to *i*-PrOAc, ketone **70** was hardly detected in the crude reaction material. Instead, vinyl

Scheme 7

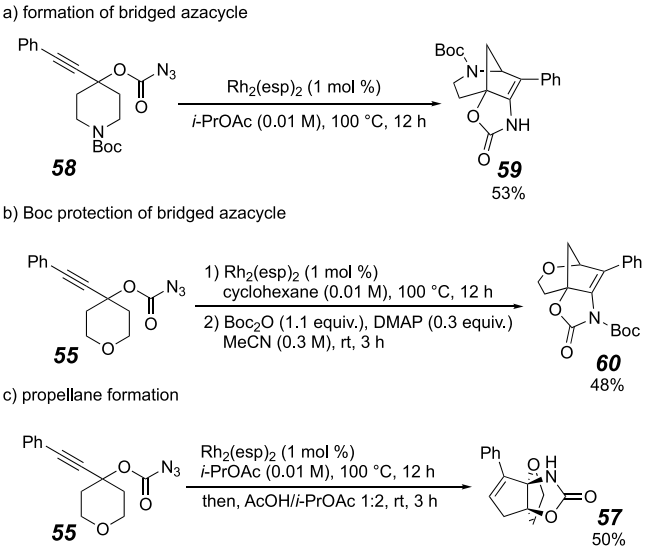

(A) Formation of Bridged Azacycle. (B) Formation of bridged azacycle. (C) Formation of a heterocyclic propellane.

imidate **72** was isolated in 34% yield.[42] Removal of the Rh catalyst gave vinyl imidate **72** as the major product in a 48% isolated yield (Scheme 9b). To further investigate this new reactivity, we prepared an acyclic carbonazidate **73** and found

https://doi.org/10.1021/acs.joc.2c00696
J. Org. Chem. XXXX, XXX, XXX−XXX

Scheme 8. Conformation Effects in the Cascade Reaction

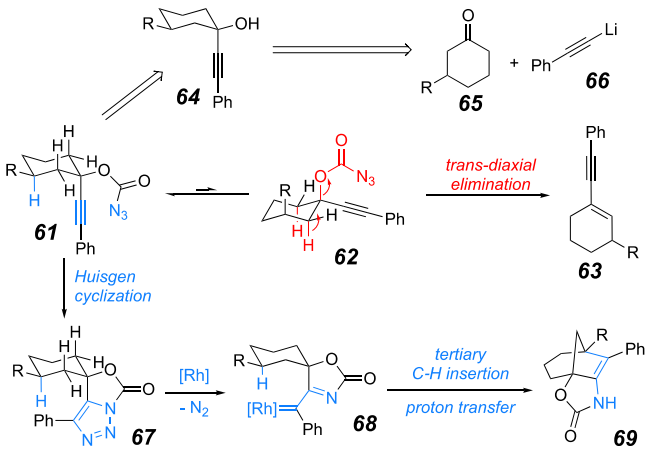

that the best condition for the formation of vinyl imidate **74** was exactly the same as bridged azacycle formation shown previously. In addition, we did not observe any fused bicyclic product **75** in this case.

Besides saturated hydrocarbon- and ester-based solvents, amide-based solvents were also examined with the expectation that their Lewis basicity would impact reactivity somewhat similarly to esters. However, amide solvents failed to give similar solvent adducts to the esters. With *N*,*N*-dimethylformamide (DMF), *N*,*N*-dimethylcarbamate **78** was obtained in a 50% yield along with 29% of propargyl alcohol **77** (Scheme 10). The carbamate product could be due to nucleophilic

Scheme 10. Outcome from Carbonazidate Reaction with Amides and DMSO

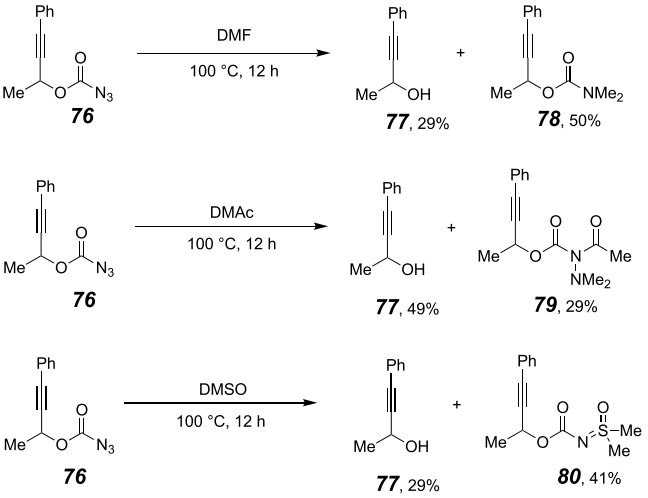

substitution by dimethylamine, which is a thermal decomposition product from DMF.[43] The propargyl alcohol byproduct has not been observed in previous transformations. Another amide solvent, *N*,*N*-dimethylacetamide (DMAc), gave propargyl alcohol **77** as the major product in a 49% yield. Additionally, an intriguing *N*,*N*-dimethyl hydrazine product **79** was isolated in a 29% yield. We propose that nitrene generation followed by C−N insertion between carbonyl and nitrogen in DMAc formed that product. A similar rhodium(II)-

Scheme 9. Effect of the Solvent on Product Formation[a]

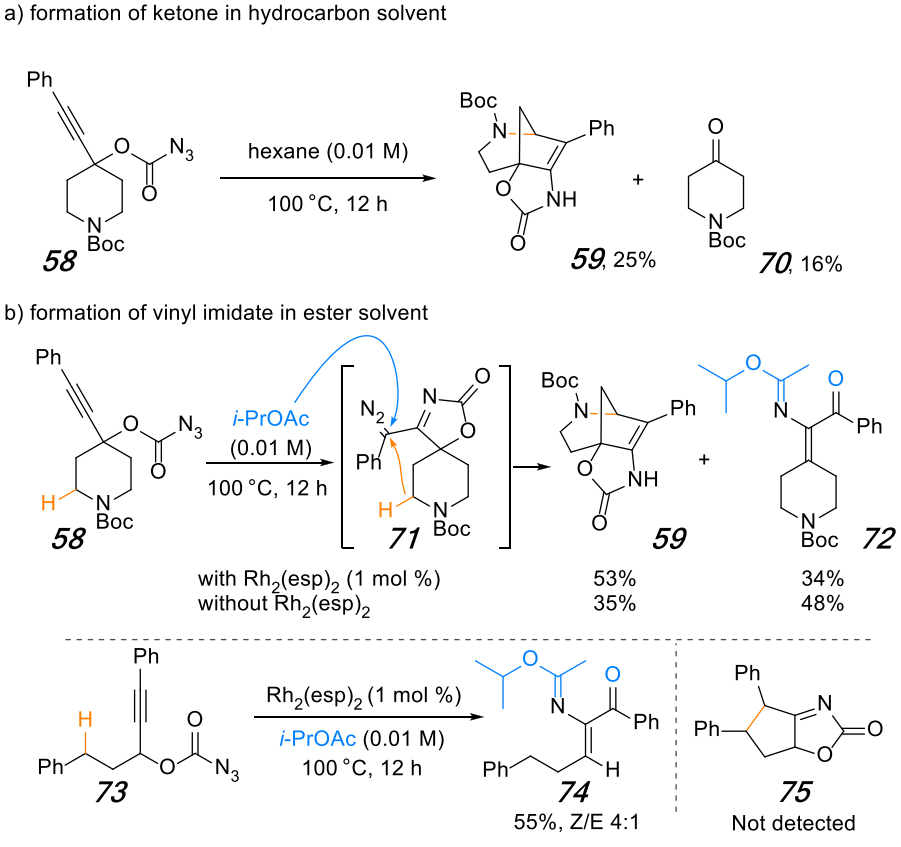

[a](A) Reaction in the hydrocarbon-based solvent. (B) Reaction in the ester-based solvent.

https://doi.org/10.1021/acs.joc.2c00696
J. Org. Chem. XXXX, XXX, XXX−XXX

Scheme 11. Metal-Catalyzed Oxidative Carbene/Alkyne Cascade Reactions[a]

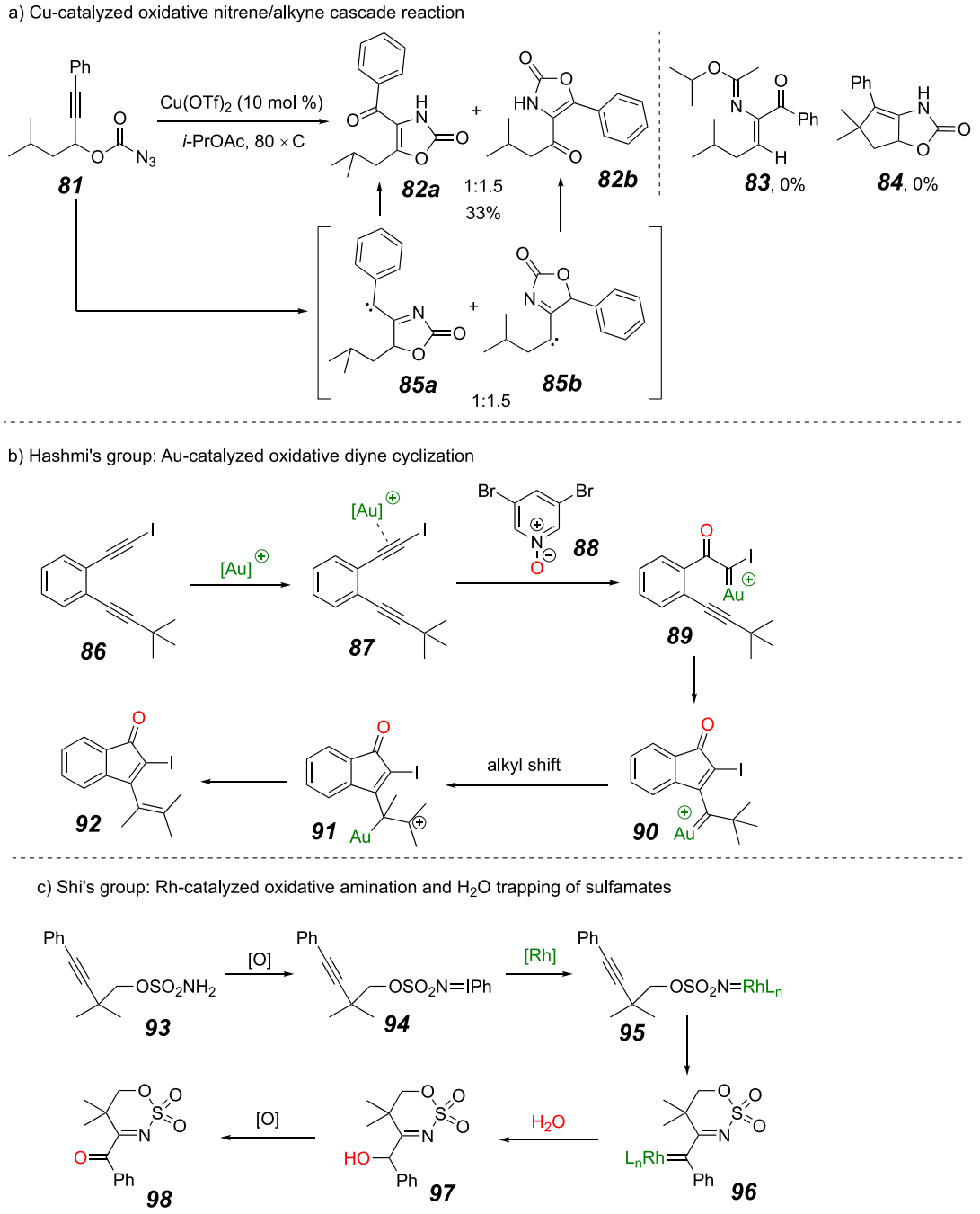

[a](A) Copper catalysis discovered in the May group. (B) Gold catalysis from Hashmi's group. (C) Rhodium catalysis from the Shi group.

catalyzed nitrene insertion into an amide C−N bond was reported by Nemoto's group in 2018,[44] which aided and supported our product structural assignment and proposed mechanism. DMSO is another common solvent in organic chemistry. When it reacted with a carbonazidate, dimethylsulfoximine **80** was isolated in 41% and 29% of propargyl alcohol **77**. The formation of dimethylsulfoximine **80** from a nitrene precursor and DMSO is a known reaction that has been published by several independent research groups.[45] Nitrene formation could result in C−O bond cleavage for formation of the propargyl alcohol. We also tried extremely anhydrous solvents with molecular sieves; however, a similar yield of propargyl alcohol was isolated. These results were all suggestive of direct generation of a nitrene from the carbonazidate instead of a Huisgen cyclization. We conclude that high-polarity aprotic solvents such as amides and sulfoxides can facilitate nitrene generation from carbonazidates. In comparison, medium-to-low-polarity aprotic solvents such as esters and hydrocarbons favored Huisgen cyclization from carbonazidates as the bridged azacycle formation and vinyl imidate formation shown above.

Investigation of Alternate Outcomes from Phenyl Alkyne-Appended Carbonazidates with Copper Catalysis. During the development of this cascade reaction, different metal catalysts were also examined. For instance, a Cu(II) catalyst gave an unusual 4-acyl-oxazolinone product

https://doi.org/10.1021/acs.joc.2c00696
J. Org. Chem. XXXX, XXX, XXX−XXX

82a and **82b** in a 33% combined yield with no formation of vinyl imidate **83** or fused bicyclic product **84** (Scheme 11a). Unlike the previously discussed Huisgen cyclization/carbene cascade reactions that required at least 100 °C for reaction initiation, this new oxidative reaction occurred at 80 °C and was complete within 12 h. This observation along with the different product distribution suggested a new reaction mechanism. The generation of acyl oxazolinone products (**82a** and **82b**) was believed to arise from oxidation of the carbene generated from a nitrene/alkyne metathesis reaction via **85a** and **85b**.

Metal-catalyzed oxidative carbene/alkyne cascade reactions have been actively developed in the past 2 decades, especially with gold catalysts.[46] For example, Hashmi's group developed a gold-catalyzed oxidative diene cyclization in 2013 (Scheme 11b).[47] The reaction was initiated by gold-catalyzed alkyne activation (**86** to **87**), followed by an oxygen transfer from a *N*-oxide **88** to form gold-bound α-oxo carbene **89**. After the second carbene/alkyne metathesis was terminated by alkyl migration, β-alkenyl enone product **92** was generated. Rhodium-catalyzed oxidative amination from sulfamates could be utilized for the synthesis of an aroyl group containing azacycles **98** via nitrene/alkyne cyclization, followed by nucleophilic trapping of in situ-generated carbene by H_2O along with oxidation (Scheme 11c).[48]

To avoid possible side reactions and simplify the product characterization, methyl alkynyl carbonazidate **76** was used for the optimization of the reaction conditions (select examples in Table 3).[49] In *i*-PrOAc, a 47% combined yield was obtained of

Table 3. Optimization of 4-Acyl-oxazolinone Formation

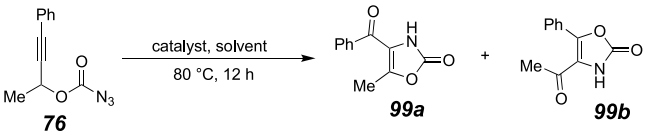

entry	catalyst and additive	solvent[a]	NMR yield[b]	ratio of **99a**:**99b**[c]
1	$Cu(OTf)_2$ (10 mol %)	*i*-PrOAc	47%	1:3.0
2	$Cu(OTf)_2$, H_2O (5 equiv)	toluene	37%	1:1.7
3	$Cu(OTf)_2$ (10 mol %)	1,4-dioxane	33%	1:2.0
4	$Cu(OTf)_2$ (10 mol %)	DMSO	63%	1:1.3
5	$Cu(OTf)_2$ (10 mol %)	DMSO[d]	62%	1:2.2
6	$Cu(OTf)_2$ (10 mol %)	DMSO[e]	64%	1:2.1
7	**$Cu(OTf)_2$ (5 mol %)**	**DMSO**	**64%**	**1:1.8**

[a]0.1 M of **76** in solvent. [b]Combined yield of **99a** and **99b** based on ^{1}H NMR peak integration relative to methyl-4-nitrobenzoate. [c]Ratio determined by ^{1}H NMR analysis of peak integration. See the Supporting Information for more details. [d]Degassed 15 min by N_2. [e]Reaction was carried out in a glovebox.

the two isomers **99a** and **99b** in a ratio of 1:3 (entry 1). Unfortunately, separating these two isomers by silica gel chromatography was infeasible. When 5 equiv of H_2O was added to toluene as a solvent, the reaction afforded **99a** and **99b** in a 37% yield (entry 2). The observation that only the starting material was recovered from the reaction in anhydrous toluene suggested that water is important in the reaction initiation. Dioxane has been an efficient solvent in some carbene reactions,[50] and a 33% combined yield was afforded in this case (entry 3). Likewise, DMSO can be used as both a solvent and an oxidant in carbene oxidation reactions.[51] Gratifyingly, undehydrated DMSO gave **99a** and **99b** in a 63% yield (entry 4). Anhydrous DMSO that had been degassed with N_2 also gave **99a** and **99b** in a 62% yield (entry 5). To further determine the active oxidant in the reaction, an NMR experiment was performed with the reagents assembled in a glovebox under near-complete anhydrous and oxygen-free conditions. Nonetheless, 64% of **99a** and **99b** were still formed (entry 6). Since this was nearly identical to previous yields (entry 4−6), this outcome supported that DMSO was also acting as the oxidant. To test the catalyst's turnover ability, both higher and lower catalyst loadings were examined, and 5 mol % of the Cu catalyst was found to be efficient enough for this transformation (entry 7).

The two isomeric products can be due to a [3,3]-sigmatropic propargyl-allenyl rearrangement. Since there is no C−H insertion product nor ester solvent adduct formation after the second carbene generation (Scheme 11a), we propose that this reaction is not initiated by Huisgen cyclization and triazole ring opening. Instead, direct nitrene generation from the carbonazidate is more likely. Water is thought to aid the nitrene generation with the Cu(II) catalyst since there was no starting carbonazidate consumed when anhydrous toluene was used (entry 5, see Supporting Information). If the reaction is initiated by Huisgen cyclization, an allenyl carbonazidate from [3,3]-sigmatropic rearrangement or a triazole formation should be observed even with anhydrous conditions. We also carefully analyzed all the products from the optimized reaction in DMSO (entry 15, Scheme 12a) and found that there was only 3% of dimethylsulfoximine **80** formation, showing that nitrene/alkyne cyclization is a faster reaction than the dimethylsulfoximine formation with Cu(II) catalysts present. To exclude the possibility that dimethylsulfoximine **80** could serve as a precursor for nitrene/alkyne cyclization or not (i.e., was an active mechanistic intermediate), dimethylsulfoximine **80** was treated with the optimized Cu-catalyzed conditions. However, no cyclized products **99a** and **99b** were detected, and all starting materials decomposed to indeterminable high-polarity products after 36 h. We also performed a solvent exchange reaction between dimethylsulfoximine **80** and DMSO-d_6. After 24 h under 100 °C, no deuterated dimethylsulfoximine **D-80** was isolated and 99% of non-deuterated dimethylsulfoximine **80** was recovered. These results illustrated that the dimethylsulfoximine is quite kinetically stable and cannot act as a nitrene precursor. A proposed mechanism that takes into account these considerations is shown in Scheme 12. First, we believe that the copper catalyst can not only facilitate nitrene generation from carbonazidate but also activate the triple bond to form copper nitrene **100a** (Scheme 12b). The propargyl nitrene **100a** then can undergo [3,3]-sigmatropic rearrangement to form allene nitrene **100b**. Both **100a** and **100b** can generate α-imino copper carbene **101a** and **101b** via *exo*-cyclization, respectively. With carbene oxidation by DMSO, the final 4-carbonyl-4-oxazolin-2-one **99a** and **99b** can be formed.

CONCLUSIONS

In conclusion, a general guide for reactivities and transformations from alkynyl carbonazidates is presented. Carbonazidates can be utilized for Huisgen cyclization/carbene alkyne cascade reactions, while other nitrene precursors proved ineffective. Different substituents on the alkyne can affect the major outcome of the reaction: (a) silanols are the major products when starting from silyl alkynyl carbonazidates; (b)

https://doi.org/10.1021/acs.joc.2c00696
J. Org. Chem. XXXX, XXX, XXX−XXX

Scheme 12

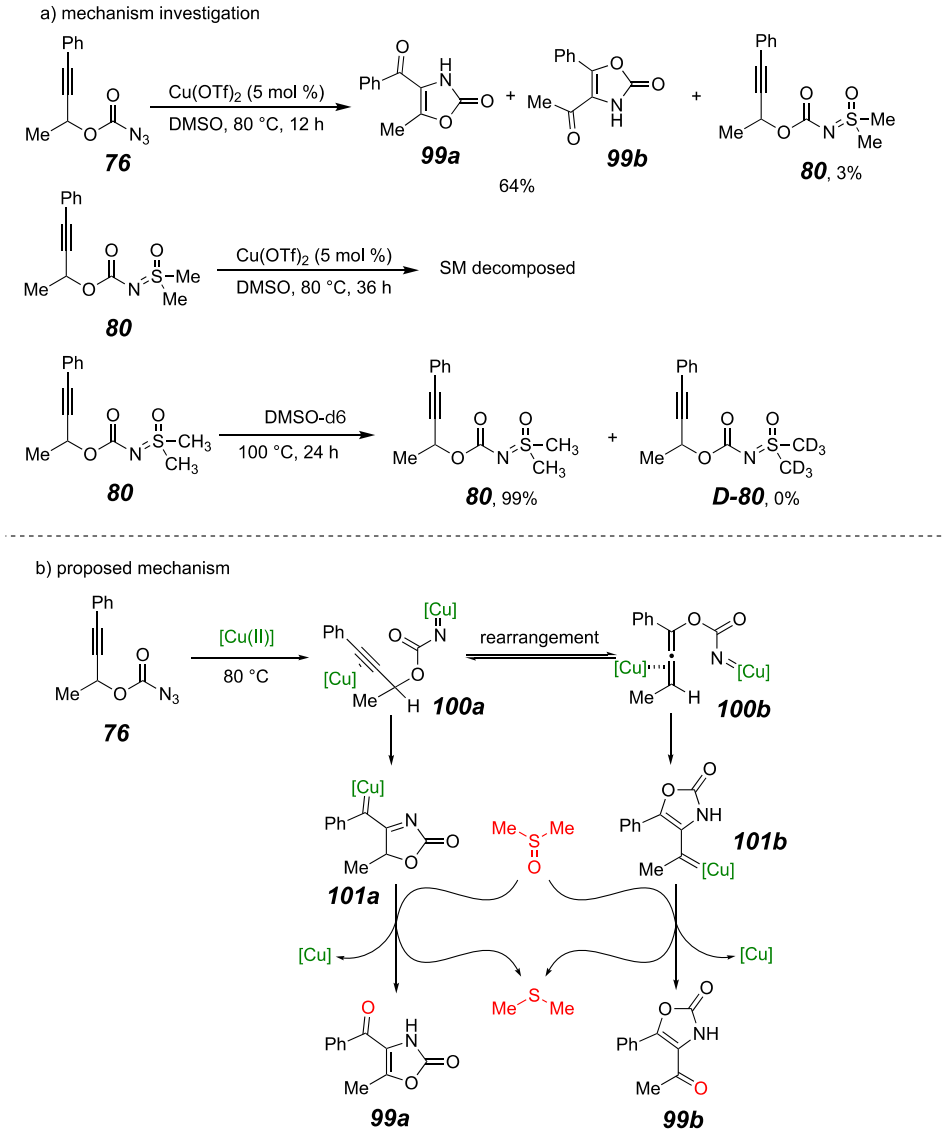

(A) Control Experiments. (B) Mechanistic consideration for 4-acyl-oxazolinone formation.

bridged azacycles become the major products when starting from aryl alkynyl carbonazidates. Computational investigation shed light on key intermediates, pointing to the likely involvement of triplet carbenes, vinylidene carbenes, and an unusual Si−N cyclobutene in the Huisgen cyclization/carbene alkyne cascade reactions. Solvents exerted great control over the reactivity of alkynyl carbonazidates. Carbonazidates in low-polarity aprotic solvents such as hydrocarbons favor Huisgen cyclization and fragmentation to a ketone as a byproduct. Medium-polarity aprotic solvents changed the major product to bridged azacycles when starting from cyclic carbonazidates or vinyl imidates when starting from acyclic carbonazidates. High-polarity aprotic solvents such as amides and DMSO can facilitate nitrene generation from the carbonazidates. In contrast to Rh(II) catalysts, Cu(II) catalysts can activate the triple bond and facilitate nitrene generation from carbonazidates, which allows an oxidative nitrene/alkyne cascade reaction to form 4-acyl-oxazolinone.

■ ASSOCIATED CONTENT

Supporting Information

The Supporting Information is available free of charge at https://pubs.acs.org/doi/10.1021/acs.joc.2c00696.

Experimental protocols, compound characterization data, catalyst analysis, reaction optimization, and computational procedures (PDF)

■ AUTHOR INFORMATION

Corresponding Authors

Dean J. Tantillo − *Department of Chemistry, University of California—Davis, Davis, California 95616, United States;* orcid.org/0000-0002-2992-8844; Email: djtantillo@ucdavis.edu

Jeremy A. May − *Department of Chemistry, University of Houston, Houston, Texas 77204-5003, United States;* orcid.org/0000-0003-3319-0077; Email: jmay@uh.edu

https://doi.org/10.1021/acs.joc.2c00696
J. Org. Chem. XXXX, XXX, XXX−XXX

Authors

Qinxuan Wang − *Department of Chemistry, University of Houston, Houston, Texas 77204-5003, United States*

Jiun-Le Shih − *Department of Chemistry, University of Houston, Houston, Texas 77204-5003, United States*

Ka Yi Tsui − *Department of Chemistry, University of California—Davis, Davis, California 95616, United States*

Croix J. Laconsay − *Department of Chemistry, University of California—Davis, Davis, California 95616, United States;* orcid.org/0000-0002-9244-1318

Complete contact information is available at: https://pubs.acs.org/10.1021/acs.joc.2c00696

Notes

The authors declare no competing financial interest.

■ ACKNOWLEDGMENTS

The NSF (grants CHE-1352439, CHE-1856416, and XSEDE) and the Welch Foundation (grant E-1744) are gratefully acknowledged for financial support.

■ REFERENCES

(1) de Frémont, P.; Marion, N.; Nolan, S. P. Carbenes: Synthesis, Properties, and Organometallic Chemistry. *Coord. Chem. Rev.* **2009**, *253*, 862−892.

(2) Ford, A.; Miel, H.; Ring, A.; Slattery, C. N.; Maguire, A. R.; McKervey, M. A. Modern Organic Synthesis with α-Diazocarbonyl Compounds. *Chem. Rev.* **2015**, *115*, 9981−10080.

(3) Kirmse, W. 100 Years of the Wolff Rearrangement. *Eur. J. Org. Chem.* **2002**, *2002*, 2193−2256.

(4) (a) Davies, H. M. L.; Antoulinakis, E. G. Intermolecular Metal-Catalyzed Carbenoid Cyclopropanations. *Org. React.* **2001**, *57*, 1−326. (b) Lebel, H.; Marcoux, J.-F.; Molinaro, C.; Charette, A. B. Stereoselective Cyclopropanation Reactions. *Chem. Rev.* **2003**, *103*, 977−1050.

(5) (a) Davies, H. M. L.; Morton, D. Guiding principles for site selective and stereoselective intermolecular C-H functionalization by donor/acceptor rhodium carbenes. *Chem. Soc. Rev.* **2011**, *40*, 1857−1869. (b) Doyle, M. P.; Duffy, R.; Ratnikov, M.; Zhou, L. Catalytic Carbene Insertion into C−H Bonds. *Chem. Rev.* **2010**, *110*, 704−724.

(6) For N−H insertion, see: (a) Hansen, S. R.; Spangler, J. E.; Hansen, J. H.; Davies, H. M. L. Metal-Free N-H Insertions of Donor/Acceptor Carbenes. *Org. Lett.* **2012**, *14*, 4626−4629. (b) Li, M.-L.; Yu, J.-H.; Li, Y.-H.; Zhu, S.-F.; Zhou, Q.-L. Highly enantioselective carbene insertion into N-H bonds of aliphatic amines. *Science* **2019**, *366*, 990−994. (c) Zhu, Y.; Liu, X.; Dong, S.; Zhou, Y.; Li, W.; Lin, L.; Feng, X. Asymmetric N−H Insertion of Secondary and Primary Anilines under the Catalysis of Palladium and Chiral Guanidine Derivatives. *Angew. Chem., Int. Ed.* **2014**, *53*, 1636−1640.

(7) For O−H insertion, see: (a) Xie, X.-L.; Zhu, S.-F.; Guo, J.-X.; Cai, Y.; Zhou, Q.-L. Enantioselective Palladium-Catalyzed Insertion of α-Aryl-α-diazoacetates into the O−H Bonds of Phenols. *Angew. Chem., Int. Ed.* **2014**, *53*, 2978−2981. (b) Tan, F.; Liu, X.; Hao, X.; Tang, Y.; Lin, L.; Feng, X. Asymmetric Catalytic Insertion of α-Diazo Carbonyl Compounds into O-H Bonds of Carboxylic Acids. *ACS Catal.* **2016**, *6*, 6930−6934. (c) San, H. H.; Wang, S.-J.; Jiang, M.; Tang, X.-Y. Boron-Catalyzed O-H Bond Insertion of α-Aryl α-Diazoesters in Water. *Org. Lett.* **2018**, *20*, 4672−4676.

(8) For Si−H and S−H insertion, see: (a) Zhang, Y.-Z.; Zhu, S.-F.; Wang, L.-X.; Zhou, Q.-L. Copper-Catalyzed Highly Enantioselective Carbenoid Insertion into Si−H Bonds. *Angew. Chem., Int. Ed.* **2008**, *47*, 8496−8498. (b) Chen, D.; Zhu, D.-X.; Xu, M.-H. Rhodium(I)-Catalyzed Highly Enantioselective Insertion of Carbenoid into Si-H: Efficient Access to Functional Chiral Silanes. *J. Am. Chem. Soc.* **2016**, *138*, 1498−1501. (c) Zhang, Y.-Z.; Zhu, S.-F.; Cai, Y.; Mao, H.-X.; Zhou, Q.-L. Copper-catalyzed enantioselective carbenoid insertion into S-H bonds. *Chem. Commun.* **2009**, 5362−5364. (d) Keipour, H.; Jalba, A.; Delage-Laurin, L.; Ollevier, T. Copper-Catalyzed Carbenoid Insertion Reactions of α-Diazoesters and α-Diazoketones into Si-H and S-H Bonds. *J. Org. Chem.* **2017**, *82*, 3000−3010. (e) Chen, K.; Zhang, S.-Q.; Brandenberg, O. F.; Hong, X.; Arnold, F. H. Alternate Heme Ligation Steers Activity and Selectivity in Engineered Cytochrome P450-Catalyzed Carbene-Transfer Reactions. *J. Am. Chem. Soc.* **2018**, *140*, 16402−16407.

(9) Reisman, S.; Nani, R.; Levin, S. Buchner and Beyond: Arene Cyclopropanation as Applied to Natural Product Total Synthesis. *Synlett* **2011**, *2011*, 2437−2442.

(10) (a) Padwa, A.; Hornbuckle, S. F. Ylide Formation from the Reaction of Carbenes and Carbenoids with Heteroatom Lone Pairs. *Chem. Rev.* **1991**, *91*, 263−309. (b) Padwa, A.; Zou, Y.; Cheng, B.; Li, H.; Downer-Riley, N.; Straub, C. S. Intramolecular Cycloaddition Reactions of Furo[3,4-b]indoles for Alkaloid Synthesis. *J. Org. Chem.* **2014**, *79*, 3173−3184. (c) Toda, Y.; Kaku, W.; Tsuruoka, M.; Shinogaki, S.; Abe, T.; Kamiya, H.; Kikuchi, A.; Itoh, K.; Suga, H. Three-Component Reactions of Diazoesters, Aldehydes, and Imines Using a Dual Catalytic System Consisting of a Rhodium(II) Complex and a Lewis Acid. *Org. Lett.* **2018**, *20*, 2659−2662. (d) Doyle, M. P.; Hu, W.; Timmons, D. J. Epoxides and Aziridines from Diazoacetates via Ylide Intermediates. *Org. Lett.* **2001**, *3*, 933−935. (e) Li, Z.; Boyarskikh, V.; Hansen, J. H.; Autschbach, J.; Musaev, D. G.; Davies, H. M. L. Scope and Mechanistic Analysis of the Enantioselective Synthesis of Allenes by Rhodium-Catalyzed Tandem Ylide Formation/[2,3]-Sigmatropic Rearrangement between Donor/Acceptor Carbenoids and Propargylic Alcohols. *J. Am. Chem. Soc.* **2012**, *134*, 15497−15504. (f) Mace, N.; Thornton, A. R.; Blakey, S. B. Unveiling Latent α-Iminocarbene Reactivity for Intermolecular Cascade Reactions through Alkyne Oxidative Amination. *Angew. Chem., Int. Ed.* **2013**, *52*, 5836−5839.

(11) Brieskorn, C. H.; Fuchs, A.; Bredenberg, J. B.-s.; McChesney, J. D.; Wenkert, E. The Structure of Carnosol. *J. Org. Chem.* **1964**, *29*, 2293−2298.

(12) (a) Li, S.-H.; Wang, J.; Niu, X.-M.; Shen, Y.-H.; Zhang, H.-J.; Sun, H.-D.; Li, M.-L.; Tian, Q.-E.; Lu, Y.; Cao, P.; Zheng, Q.-T. Maoecrystal V, Cytotoxic Diterpenoid with a Novel C19 Skeleton from Isodon eriocalyx (Dunn.) Hara. *Org. Lett.* **2004**, *6*, 4327−4330. (b) Jansone-Popova, S.; May, J. A. Stereoelectronic factors in bridgehead C-H bond insertion: studies toward the total synthesis of maoecrystal V. *Tetrahedron Lett.* **2016**, *72*, 3734−3747.

(13) (a) Evanno, L.; Jossang, A.; Nguyen-Pouplin, J.; Delaroche, D.; Herson, P.; Seuleiman, M.; Bodo, B.; Nay, B. Further Studies of the Norditerpene (+)-Harringtonolide Isolated fromCephalotaxus harringtoniavar.drupacea: Absolute Configuration, Cytotoxic and Antifungal Activities. *Planta Med.* **2008**, *74*, 870−872. (b) Buta, J. G.; Flippen, J. L.; Lusby, W. R. Harringtonolide, a plant growth inhibitory tropone from Cephalotaxus harringtonia (Forbes) K. Koch. *J. Org. Chem.* **1978**, *43*, 1002−1003. (c) Zhang, H.-J.; Hu, L.; Ma, Z.; Li, R.; Zhang, Z.; Tao, C.; Cheng, B.; Li, Y.; Wang, H.; Zhai, H. Total Synthesis of the Diterpenoid (+)-Harringtonolide. *Angew. Chem., Int. Ed.* **2016**, *55*, 11638−11641.

(14) George, J. H.; Hesse, M. D.; Baldwin, J. E.; Adlington, R. M. Biomimetic Synthesis of Polycyclic Polyprenylated Acylphloroglucinol Natural Products Isolated from Hypericum papuanum. *Org. Lett.* **2010**, *12*, 3532−3535.

(15) Ghosh, A.; Carter, R. G. Recent Syntheses and Strategies toward Polycyclic Gelsemium Alkaloids. *Angew. Chem., Int. Ed.* **2019**, *58*, 681−694.

(16) (a) Wiberg, K. B. Small Ring Propellanes. *Chem. Rev.* **1989**, *89*, 975−983. (b) Pihko, A. J.; Koskinen, A. M. P. Synthesis of propellane-containing natural products. *Tetrahedron Lett.* **2005**, *61*, 8769−8807.

(17) Yang, B. O.; Ke, C.-Q.; He, Z.-S.; Yang, Y.-P.; Ye, Y. Brazilide A, a novel lactone with an unprecedented skeleton from Caesalpinia sappan. *Tetrahedron Lett.* **2002**, *43*, 1731−1733.

(18) Gao, Y.; Fan, M.; Geng, Q.; Ma, D. Total Synthesis of Lapidilectine B Enabled by Manganese(III)-Mediated Oxidative Cyclization of Indoles. *Chem.—Eur. J.* **2018**, *24*, 6547−6550.

(19) (a) Miura, Y.; Hayashi, N.; Yokoshima, S.; Fukuyama, T. Total Synthesis of (−)-Isoschizogamine. *J. Am. Chem. Soc.* **2012**, *134*, 11995−11997. (b) Xu, Z.; Bao, X.; Wang, Q.; Zhu, J. An Enantioselective Total Synthesis of (−)-Isoschizogamine. *Angew. Chem., Int. Ed.* **2015**, *54*, 14937−14940.
(20) Kurosu, M.; Marcin, L. R.; Grinsteiner, T. J.; Kishi, Y. Total Synthesis of (±)-Batrachotoxinin A. *J. Am. Chem. Soc.* **1998**, *120*, 6627−6628.
(21) (a) Gong, J.; Lin, G.; Sun, W.; Li, C.-C.; Yang, Z. Total Synthesis of (±) Maoecrystal V. *J. Am. Chem. Soc.* **2010**, *132*, 16745−16746. (b) Peng, F.; Danishefsky, S. J. Total Synthesis of (±)-Maoecrystal V. *J. Am. Chem. Soc.* **2012**, *134*, 18860−18867. (c) Lu, P.; Gu, Z.; Zakarian, A. Total Synthesis of Maoecrystal V: Early-Stage C-H Functionalization and Lactone Assembly by Radical Cyclization. *J. Am. Chem. Soc.* **2013**, *135*, 14552−14555. (d) Lu, P.; Mailyan, A.; Gu, Z.; Guptill, D. M.; Wang, H.; Davies, H. M. L.; Zakarian, A. Enantioselective Synthesis of (−)-Maoecrystal V by Enantiodetermining C-H Functionalization. *J. Am. Chem. Soc.* **2014**, *136*, 17738−17749. (e) Zheng, C.; Dubovyk, I.; Lazarski, K. E.; Thomson, R. J. Enantioselective Total Synthesis of (−)-Maoecrystal V. *J. Am. Chem. Soc.* **2014**, *136*, 17750−17756.
(22) (a) Jansone-Popova, S.; May, J. A. Synthesis of Bridged Polycyclic Ring Systems via Carbene Cascades Terminating in C-H Bond Insertion. *J. Am. Chem. Soc.* **2012**, *134*, 17877−17880. (b) Jansone-Popova, S.; Le, P. Q.; May, J. A. Carbene cascades for the formation of bridged polycyclic rings. *Tetrahedron* **2014**, *70*, 4118−4127. (c) Le, P. Q.; May, J. A. Hydrazone-Initiated Carbene/Alkyne Cascades to Form Polycyclic Products: Ring-Fused Cyclopropenes as Mechanistic Intermediates. *J. Am. Chem. Soc.* **2015**, *137*, 12219−12222. (d) Wang, Q.; May, J. A. Synthesis of Bridged Azacycles and Propellanes via Nitrene/Alkyne Cascades. *Org. Lett.* **2020**, *22*, 3039−3044.
(23) (a) Korkowski, P. F.; Hoye, T. R.; Rydberg, D. B. Fischer carbene-mediated conversions of enynes to bi- and tricyclic cyclopropane-containing carbon skeletons. *J. Am. Chem. Soc.* **1988**, *110*, 2676−2678. (b) Padwa, A.; Krumpe, K. E.; Zhi, L. Cycloalkenone formation by the intramolecular addition of a α-diazoketone to an acetylenic pi-bond. *Tetrahedron Lett.* **1989**, *30*, 2633−2636. (c) Zhang, C.; Li, H.; Pei, C.; Qiu, L.; Hu, W.; Bao, X.; Xu, X. Selective Vinylogous Reactivity of Carbene Intermediate in Gold-Catalyzed Alkyne Carbocyclization: Synthesis of Indenols. *ACS Catal.* **2019**, *9*, 2440−2447. (d) Zhu, D.; Chen, L.; Zhang, H.; Ma, Z.; Jiang, H.; Zhu, S. Highly Chemo- and Stereoselective Catalyst-Controlled Allylic C−H Insertion and Cyclopropanation Using Donor/Donor Carbenes. *Angew. Chem., Int. Ed.* **2018**, *57*, 12405−12409. (e) Wang, X.; Abrahams, Q. M.; Zavalij, P. Y.; Doyle, M. P. Highly Regio- and Stereoselective Dirhodium Vinylcarbene Induced Nitrone Cycloaddition with Subsequent Cascade Carbenoid Aromatic Cycloaddition/N−O Cleavage and Rearrangement. *Angew. Chem., Int. Ed.* **2012**, *51*, 5907−5910.
(24) (a) Thornton, A. R.; Blakey, S. B. Catalytic Metallonitrene/Alkyne Metathesis: A Powerful Cascade Process for the Synthesis of Nitrogen-Containing Molecules. *J. Am. Chem. Soc.* **2008**, *130*, 5020−5021. (b) Thornton, A. R.; Martin, V. I.; Blakey, S. B. π-Nucleophile Traps for Metallonitrene/Alkyne Cascade Reactions: A Versatile Process for the Synthesis of α-Aminocyclopropanes and β-Aminostyrenes. *J. Am. Chem. Soc.* **2009**, *131*, 2434−2435. (c) Mace, N.; Thornton, A. R.; Blakey, S. B. Unveiling Latent α-Iminocarbene Reactivity for Intermolecular Cascade Reactions through Alkyne Oxidative Amination. *Angew. Chem., Int. Ed.* **2013**, *52*, 5836−5839.
(25) Please see the Supporting Information for Experimental Methods.
(26) Frisch, M. J.; Trucks, G. W.; Schlegel, H. B.; Scuseria, G. E.; Robb, M. A.; Cheeseman, J. R.; Scalmani, G.; Barone, V.; Petersson, G. A.; Nakatsuji, H.; Li, X.; Caricato, M.; Marenich, A. V.; Bloino, J.; Janesko, B. G.; Gomperts, R.; Mennucci, B.; Hratchian, H. P.; Ortiz, J. V.; Izmaylov, A. F.; Sonnenberg, J. L.; Williams-Young, D.; Ding, F.; Lipparini, F.; Egidi, F.; Goings, J.; Peng, B.; Petrone, A.; Henderson, T.; Ranasinghe, D.; Zakrzewski, V. G.; Gao, J.; Rega, N.; Zheng, G.; Liang, W.; Hada, M.; Ehara, M.; Toyota, K.; Fukuda, R.; Hasegawa, J.; Ishida, M.; Nakajima, T.; Honda, Y.; Kitao, O.; Nakai, H.; Vreven, T.; Throssell, K.; Montgomery, Jr., J. A.; Peralta, J. E.; Ogliaro, F.; Bearpark, M. J.; Heyd, J. J.; Brothers, E. N.; Kudin, K. N.; Staroverov, V. N.; Keith, T. A.; Kobayashi, R.; Normand, J.; Raghavachari, K.; Rendell, A. P.; Burant, J. C.; Iyengar, S. S.; Tomasi, J.; Cossi, M.; Millam, J. M.; Klene, M.; Adamo, C.; Cammi, R.; Ochterski, J. W.; Martin, R. L.; Morokuma, K.; Farkas, O.; Foresman, J. B.; Fox, D. J. *Gaussian 16*, Revision C.01; Gaussian, Inc.: Wallingford CT, 2016.
(27) (a) Tomasi, J.; Mennucci, B.; Cammi, R. Quantum Mechanical Continuum Solvation Models. *Chem. Rev.* **2005**, *105*, 2999−3094. (b) *Computational Chemistry: Reviews of Current Trends*; Leszczynski, J., Ed.; World Scientific Publishing Co. Pte. Ltd.: Singapore, 2003; Vol. *8*.
(28) Mardirossian, N.; Head-Gordon, M. ωB97X-V: A 10-parameter, range-separated hybrid, generalized gradient approximation density functional with nonlocal correlation, designed by a survival-of-the-fittest strategy. *Phys. Chem. Chem. Phys.* **2014**, *16*, 9904−9924.
(29) (a) Fukui, K. The Path of Chemical Reactions - the IRC Approach. *Acc. Chem. Res.* **1981**, *14*, 363−368. (b) Gonzalez, C.; Schlegel, H. B. Reaction Path Following in Mass-Weighted Internal Coordinates. *J. Phys. Chem.* **1990**, *94*, 5523−5527.
(30) Pan, D.; Wei, Y.; Shi, M. Rh(II)-Catalyzed Chemoselective Oxidative Amination and Cyclization Cascade of 1-(Arylethynyl)-cycloalkyl)methyl Sulfamates. *Org. Lett.* **2017**, *19*, 3584−3587.
(31) Shih, J.-L.; Jansone-Popova, S.; Huynh, C.; May, J. A. Synthesis of azasilacyclopentenes and silanols via Huisgen cycloaddition-initiated C-H bond insertion cascades. *Chem. Sci.* **2017**, *8*, 7132−7137.
(32) (a) Davidson, E. R. In *Diradicals*; Borden, W. T., Ed.; Wiley-Interscience: New York, 1982; p. 73; (b) Schaefer, H. F., III Methylene: A Paradigm for Computational Quantum Chemistry. *Science* **1986**, *231*, 1100−1107. (c) Riplinger, C.; Pinski, P.; Becker, U.; Valeev, E. F.; Neese, F. Sparse maps-A systematic infrastructure for reduced-scaling electronic structure methods. II. Linear scaling domain based pair natural orbital coupled cluster theory. *J. Chem. Phys.* **2016**, *144*, 024109.
(33) (a) Baker, J.; Scheiner, A.; Andzelm, J. Spin Contamination in Density Functional Theory. *Chem. Phys. Lett.* **1993**, *216*, 380−388. (b) Cramer, C. J.; Dulles, F. J.; Falvey, D. E. Ab Initio Characterization of Phenylnitrenium and Phenylcarbene: Remarkably Different Properties for Isoelectronic Species. *J. Am. Chem. Soc.* **1994**, *116*, 9787−9788.
(34) Henkel, S.; Costa, P.; Klute, L.; Sokkar, P.; Fernandez-Oliva, M.; Thiel, W.; Sanchez-Garcia, E.; Sander, W. Switching the Spin State of Diphenylcarbene Via Halogen Bonding. *J. Am. Chem. Soc.* **2016**, *138*, 1689−1697.
(35) (a) Ross, J. A.; Seiders, R. P.; Lemal, D. M. An extraordinarily facile sulfoxide automerization. *J. Am. Chem. Soc.* **1976**, *98*, 4325−4327. (b) Birney, D. M.; Ham, S.; Unruh, G. R. Pericyclic and Pseudopericyclic Thermal Cheletropic Decarbonylations: When Can a Pericyclic Reaction Have a Planar, Pseudopericyclic Transition State?1. *J. Am. Chem. Soc.* **1997**, *119*, 4509−4517. (c) Birney, D. M. Theory, Experiment and Unusual Features of Potential Energy Surfaces of Pericyclic and Pseudopericyclic Reactions with Sequential Transition Structures. *Curr. Org. Chem.* **2010**, *14*, 1658−1668. (d) Lemal, D. M. Chemistry of Hexafluorobicyclo[1.1.0]butane: A Computational Study,. *J. Org. Chem.* **2010**, *75*, 6411−6415. (e) Hare, S. R.; Tantillo, D. J. Pericyclic or Pseudopericyclic? The Case of an Allylic Transposition in the Synthesis of a Saccharin Derivative. *J. Chem. Educ.* **2017**, *94*, 988−993.
(36) Qin, Y.; Lu, B.; Rauhut, G.; Hagedorn, M.; Banert, K.; Song, C.; Chu, X.; Wang, L.; Zeng, X. The Simplest, Isolable, Alkynyl Isocyanate HC≡CNCO: Synthesis and Characterization. *Angew. Chem., Int. Ed.* **2019**, *58*, 17277−17281.
(37) (a) Vrtilek, J. M.; Gottlieb, C. A.; Langer, W. D.; Thaddeus, P.; Wilson, R. W. Laboratory and Astronomical Detection of the Deuterated Ethynyl Radical CCD. *Astrophys. J.* **1985**, *296*, L35−

https://doi.org/10.1021/acs.joc.2c00696
J. Org. Chem. XXXX, XXX, XXX−XXX

L38. (b) Pasinszki, T.; Havasi, B. Quantum-chemical study of the structure and stability of ethynyl pseudohalides: HC≡C-NCO and its isomers. *Phys. Chem. Chem. Phys.* **2003**, *5*, 259−267. (c) Lattanzi, V.; Gottlieb, C. A.; Thaddeus, P.; Thorwirth, S.; McCarthy, M. C. THE ROTATIONAL SPECTRUM OF THE NCO-ANION. *Astrophys. J.* **2010**, *720*, 1717−1720. (d) Fourré, I.; Matz, O.; Ellinger, Y.; Guillemin, J.-C. Relative Thermodynamic Stability of the [C,N,O] Linkages as an Indication of the Most Abundant Structures in the ISM. *Astron. Astrophys.* **2020**, *639*, A16.

(38) (a) Annadi, K.; Wee, A. G. H. An Alkylidene Carbene C-H Activation Approach toward the Enantioselective Syntheses of Spirolactams: Application to the Synthesis of (−)-Adalinine. *J. Org. Chem.* **2016**, *81*, 1021−1038. (b) Pietruszka, J.; Witt, A. Synthesis of the Bestmann-Ohira Reagent. *Synthesis* **2006**, *2006*, 4266−4268.

(39) (a) Calad, S. A.; Woerpel, K. A. Silylene Transfer to Carbonyl Compounds and Subsequent Ireland−Claisen Rearrangements to Control Formation of Quaternary Carbon Stereocenters. *J. Am. Chem. Soc.* **2005**, *127*, 2046−2047. (b) Brückmann, R.; Maas, G. Thermal Decomposition of α-Diazo-α-(trialkylsilyl)alkanones - Intramolecular C/H Insertion of Siloxyalkylidenecarbene Intermediates. *Chem. Ber.* **1987**, *120*, 635−641.

(40) Kevy, G. C.; Lichter, R. L. *Nitrogen-15 Nuclear Magnetic Resonance Spectroscopy*; J. Wiley: New York, NY, 1979.

(41) (a) Dewyer, A. L.; Argüelles, A. J.; Zimmerman, P. M. Methods for Exploring Reaction Space in Molecular Systems. *Wiley Interdiscip. Rev. Comput. Mol. Sci.* **2018**, *8*, No. e1354. (b) Simm, G. N.; Vaucher, A. C.; Reiher, M. Exploration of Reaction Pathways and Chemical Transformation Networks. *J. Phys. Chem. A* **2019**, *123*, 385−399. (c) Unsleber, J. P.; Reiher, M. The Exploration of Chemical Reaction Networks. *Annu. Rev. Phys. Chem.* **2020**, *71*, 121−142. (d) Wang, L.-P.; Titov, A.; McGibbon, R.; Liu, F.; Pande, V. S.; Martínez, T. J. Discovering Chemistry with an ab initio Nanoreactor. *Nat. Chem.* **2014**, *6*, 1044−1048. (e) Rappoport, D.; Aspuru-Guzik, A. Predicting Feasible Organic Reaction Pathways Using Heuristically Aided Quantum Chemistry. *J. Chem. Theory Comput.* **2019**, *15*, 4099−4112.

(42) Wang, Q.; May, J. A. Formation of β-Oxo-N-vinylimidates via Intermolecular Ester Incorporation in Huisgen Cyclization/Carbene Cascade Reactions. *Org. Lett.* **2020**, *22*, 9579−9584.

(43) Heravi, M. M.; Ghavidel, M.; Mohammadkhani, L. Beyond a Solvent: Triple Roles of Dimethylformamide in Organic Chemistry. *RSC Adv.* **2018**, *8*, 27832−27862.

(44) Kono, M.; Harada, S.; Nemoto, T. Chemoselective Intramolecular Formal Insertion Reaction of Rh−Nitrenes into an Amide Bond Over C−H Insertion. *Chem.—Eur. J.* **2019**, *25*, 3119−3124.

(45) (a) Kirby, G. W.; Mackinnon, J. W. M.; Sharma, R. P. Reaction of Alkoxycarbonylnitrenes with Dimethyl Sulphoxide; Formation of Transient Nitrosoformates. *Tetrahedron Lett.* **1977**, *18*, 215−218. (b) Leca, D.; Toussaint, A.; Mareau, C.; Fensterbank, L.; Lacôte, E.; Malacria, M. Efficient Copper-Mediated Reactions of Nitrenes Derived from Sulfonimidamides. *Org. Lett.* **2004**, *6*, 3573−3575.

(46) Zheng, Z.; Wang, Z.; Wang, Y.; Zhang, L. Au-Catalysed Oxidative Cyclisation. *Chem. Soc. Rev.* **2016**, *45*, 4448−4458.

(47) Nösel, P.; dos Santos Comprido, L. N.; Lauterbach, T.; Rudolph, M.; Rominger, F.; Hashmi, A. S. 1,6-Carbene Transfer: Gold-Catalyzed Oxidative Diyne Cyclizations. *J. Am. Chem. Soc.* **2013**, *135*, 15662−15666.

(48) Pan, D.; Wei, Y.; Shi, M. Rh(II)-Catalyzed Chemoselective Oxidative Amination and Nucleophilic Trapping of gem-Dimethyl Alkynyl-Tethered Sulfamates. *Org. Lett.* **2018**, *20*, 84−87.

(49) See the Supporting Information for full details.

(50) Le, P. Q.; May, J. A. Hydrazone-Initiated Carbene/Alkyne Cascades to Form Polycyclic Products: Ring-Fused Cyclopropenes as Mechanistic Intermediates. *J. Am. Chem. Soc.* **2015**, *137*, 12219−12222.

(51) (a) O'Connor, N. R.; Bolgar, P.; Stoltz, B. M. Development of a Simple System for the Oxidation of Electron-Rich Diazo Compounds to Ketones. *Tetrahedron Lett.* **2016**, *57*, 849−851. (b) Bakulev, V. A.; Tarasov, E. V.; Morzherin, Y. Y.; Luyten, I.; Toppet, S.; Dehaen, W. Synthesis and Study of the Rearrangements of 5-(1,2,3-Triazol-4-Yl)-1,2,3-Thiadiazoles. *Tetrahedron* **1998**, *54*, 8501−8514.

https://doi.org/10.1021/acs.joc.2c00696
J. Org. Chem. XXXX, XXX, XXX−XXX